

Alma Mater Studiorum – Università di Bologna



**DOTTORATO DI RICERCA IN BIOLOGIA CELLULARE E
MOLECOLARE**

Ciclo XXVI

Settore Concorsuale di afferenza: 05/E2

Settore Scientifico disciplinare: BIO/11

**Analysis of Two Component Systems in Group B *Streptococcus*
Shows that RgfAC and the Novel FspSR Modulate Virulence and
Bacterial Fitness**

Presentata da: Cristina Faralla

Coordinatore Dottorato

Ch.mo Prof. Vincenzo Scarlato

Relatori

Ch.mo Prof. Vincenzo Scarlato

Dott. Robert Janulczyk

Esame finale anno 2014

*Nobody said it would be easy, they just promised it
would most likely be worth it*

— Harvey MacKay

*Al mio amato nonno Rosario,
che sarebbe stato fiero di vedermi raggiungere questo traguardo.*

*Ai miei genitori Massimo e Sissi,
perché è grazie al loro costante supporto e sostegno che sono qui oggi.*

*Alle mie sorelle Ida e Federica,
perché non smettano mai di creder in loro stesse e possano realizzare
tutti i loro sogni.*

Il mio progetto di dottorato, presentato in questo lavoro di tesi, si è focalizzato sullo studio dei sistemi a due componenti in *Streptococcus agalactiae*. Tali sistemi agiscono da sensori per il batterio percependo particolari stimoli ambientali e attivando di conseguenza una risposta intracellulare specifica (spesso di tipo trascrizionale). Essi rappresentano quindi uno strumento indispensabile per l'adattamento, la sopravvivenza e la patogenesi dei batteri.

Nel presente lavoro, mediante un approccio combinato di bioinformatica e analisi trascrizionale, cinque sistemi, precedentemente poco o per nulla caratterizzati, sono stati scelti come target di studio. Mutanti di delezione in ognuno dei cinque sistemi sono stati quindi ottenuti in *S. agalactiae* e caratterizzati sia *in vitro* che *in vivo*. I risultati di tale studio sono riportati nella seguente tesi ed in un articolo attualmente in revisione dalla rivista MBio.

Faralla C, Metruccio MM, De Chiara M*, Mu R. *, Patras KA*, Muzzi A, Grandi G, Margarit I, Doran KS, Janulczyk R. *Analysis of two component systems in Group B Streptococcus shows that RgfAC and the novel FspSR modulate virulence and bacterial fitness.*

Under Review-MBio

*Questi autori hanno contribuito ugualmente al presente lavoro.

Parallelamente a questo progetto ho anche collaborato alla caratterizzazione immunologica e funzionale di uno degli antigeni scelti come candidato vaccino

contro *Streptococcus pyogenes* dalla Novartis Vaccines & Diagnostic di Siena. In particolare, mi sono occupata della generazione di ceppi ricombinanti di *S.pyogenes* in cui la Streptolisina-O fosse assente o sostituita con una sua forma mutata. I ceppi generati sono stati quindi caratterizzati *in vivo* al fine di investigare come questa proteina fosse coinvolta nell'evasione della risposta immunitaria da parte del batterio. Il lavoro svolto è stato oggetto di una pubblicazione scientifica.

Chiarot E, **Faralla C**, Chiappini N, Tuscano G, Falugi F, Gambellini G, Taddei A, Capo S, Cartocci E, Veggi D, Corrado A, Mangiavacchi S, Tavarini S, Scarselli M, Janulczyk R, Grandi G, Margarit I, Bensi G. *Targeted amino Acid substitutions impair streptolysin o toxicity and Group A Streptococcus virulence*. MBio. 2013 Jan 8;4(1).

Abstract

Group B *Streptococcus* (GBS), in its transition from commensal to pathogen, will encounter diverse host environments and thus require coordinately controlling its transcriptional responses to these changes. This work was aimed at better understanding the role of two component signal transduction systems (TCS) in GBS pathophysiology through a systematic screening procedure. We first performed a complete inventory and sensory mechanism classification of all putative GBS TCS by genomic analysis. Five TCS were further investigated by the generation of knock-out strains, and *in vitro* transcriptome analysis identified genes regulated by these systems, ranging from 0.1-3% of the genome. Interestingly, two sugar phosphotransferase systems appeared differently regulated in the knock-out mutant of TCS-16, suggesting an involvement in monitoring carbon source availability. High throughput analysis of bacterial growth on different carbon sources showed that TCS-16 was necessary for growth of GBS on fructose-6-phosphate. Additional transcriptional analysis provided further evidence for a stimulus-response circuit where extracellular fructose-6-phosphate leads to autoinduction of TCS-16 with concomitant dramatic up-regulation of the adjacent operon encoding a phosphotransferase system. The TCS-16-deficient strain exhibited decreased persistence in a model of vaginal colonization and impaired growth/survival in the presence of vaginal mucoid components. All mutant strains were also characterized in a murine model of systemic infection, and inactivation of TCS-17 (also known as RgfAC) resulted in hypervirulence. Our data suggest a role for the previously

unknown TCS-16, here named FspSR, in bacterial fitness and carbon metabolism during host colonization, and also provide experimental evidence for TCS-17/RgfAC involvement in virulence.

Table of Contents

1. Introduction.....	8
1.1. <i>Streptococcus agalactiae</i>.....	8
1.2. Two component systems.....	11
1.3. Two component systems in GBS.....	13
1.4. Aim of the study and importance.....	14
2. Results.....	16
2.1. Identification and comparative genomics of TCS.....	16
2.2. Domain architecture for TCS in the genome of CJB11.....	20
2.3. Transcriptional analysis of TCS.....	22
2.4. Expression microarray analysis of TCS mutants.....	24
2.5. Phenotype microarray screening shows that TCS-16 influences carbon source utilization.....	30
2.6. TCS-16 gene regulation in response to extracellular Fru-6- P.....	33
2.7. The RR16 recombinant protein is insoluble when expressed in <i>E. coli</i>.....	36
2.8. TCS-16 influences vaginal persistence in mice.....	40

2.9.	TCS-17/RgfAC influences virulence in a murine model of systemic infection.....	43
2.10.	TCS-17/RgfAC shows higher duplication rate in human blood.....	45
3.	Discussion.....	48
4.	Materials and Methods.....	53
4.1.	Bacterial strains and growth conditions.....	53
4.2.	Construction of TCS isogenic mutants.....	53
4.3.	Recombinant RR16 cloning, expression and purification.....	55
4.4.	Bioinformatics methods.....	57
4.5.	Expression microarray analysis.....	58
4.6.	qRT-PCR analysis.....	60
4.7.	Phenotype Microarray analysis.....	61
4.8.	<i>In vivo</i> infection experiments.....	62
4.9.	<i>In vitro</i> infection experiments.....	62
4.10.	<i>Ex vivo</i> GBS growth experiments.....	63
4.11.	Oligo list.....	65
5.	References.....	67

1. Introduction

1.1 *Streptococcus agalactiae*

Streptococcus agalactiae or Group B *Streptococcus* (GBS) is a β -hemolytic Gram-positive bacterium first recorded as cause of fatal puerperal sepsis in 1938 (1). This microorganism remained then unknown until the 1970s, when it was indicated as responsible of a dramatic increase in the incidence of septicemia and meningitis in neonates (2-4). GBS was known to cause bovine mastitis before being appreciated as



FIG 1 Coloured scanning electron micrography (SEM) of *Streptococcus agalactiae*

pathogenic in humans (5), even if substantial biochemical, serologic, and molecular differences exist between human and bovine isolates (5). In this decade, GBS remains the dominant cause of infant morbidity and mortality in the United States (6), and has also been recognized as an important cause of infections in immunocompromised patients and the elderly (7).

GBS expresses a capsular polysaccharide (CPS) that is a major virulence factor contributing to evasion of host immune defense mechanisms (8). GBS CPS can be divided into ten serotypes (Ia, Ib, II–IX), each with unique structural and antigenic features. Nevertheless, all the GBS CPS repeating units share a critical conserved element: a terminally capped sialic acid (Sia). Sia is a nine-carbon backbone sugar present abundantly in the surface glycocalyx of all mammalian cells, and in this manner GBS decorates its surface with a common host epitope – a form of molecular mimicry. The sialylated CPS is recognized as a critical factor for GBS survival *in vivo* (9), interfering with host complement system functions to block C3b deposition and limit C5a production (10, 11).

A number of additional virulence factors that are important for GBS adherence, invasion of host cells and evasion of host immunity have been described (β -hemolysin/cytolysin, CAMP factor, superoxide dismutase, pili, C5 α peptidase, serine proteinase, AMP) (12). Despite these advances, one area that deserves greater attention is how the pathogen regulates expression of these virulence factors during infection. GBS is a commensal in the rectovaginal tract of 20–30% of healthy women (13). However, by vertical transmission intrapartum, it may transition to an invasive pathogen, resulting in pneumonia, sepsis and meningitis (14). The physiopathology of GBS infections implies that this bacterium encounters several very different microenvironments during colonization and the infectious process. This indicates that GBS is efficiently able to adapt to changing host environments (Fig. 2). The

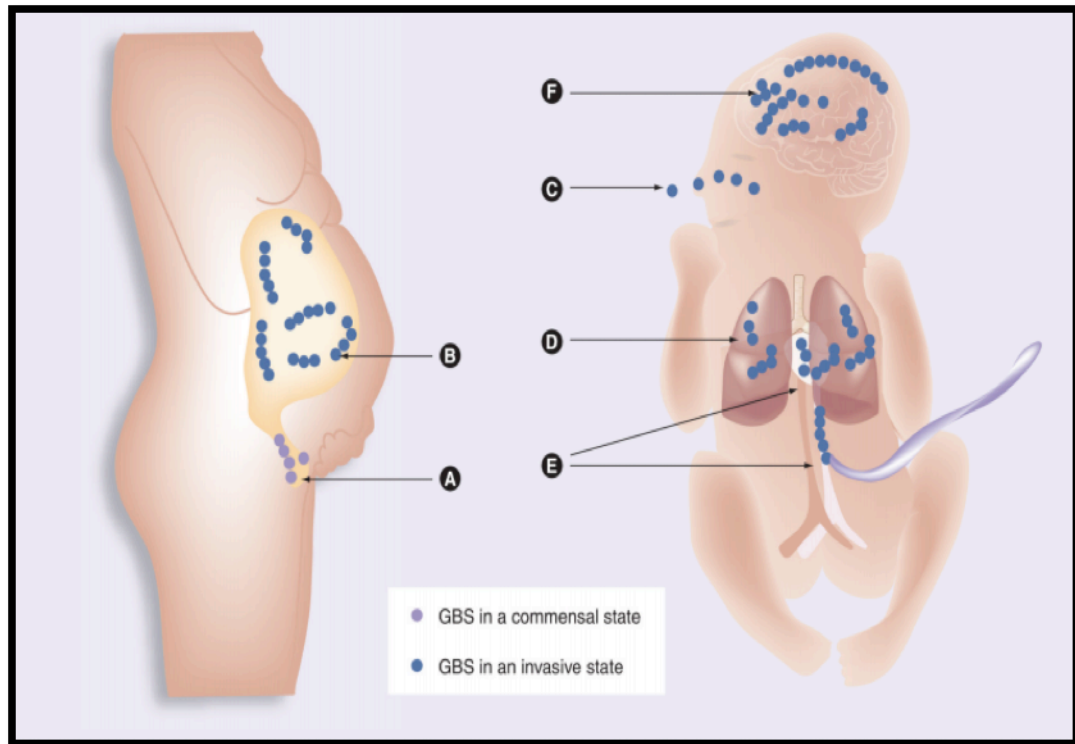


FIG 2. Lifecycle of Group B Streptococci as a neonatal pathogen. **(A)** GBS reside as a commensal in genital and lower gastrointestinal tracts of women. **(B)** GBS can infiltrate the intrauterine compartment in pregnant mothers who are asymptomatic carriers. **(C)** Newborn aspirate GBS in utero or during birth. **(D)** GBS invades the neonatal lung causing pneumonia. **(E)** From the lung, GBS gains access into the bloodstream of the neonate causing sepsis and invades multiple neonatal organs including the heart **(F)** GBS penetrates the blood brain barrier causing meningitis (12).

transition of the organism from a commensal niche (e.g. vaginal tract) to invasive niches (e.g. blood, lung, brain, and other organs) is likely to require adaptive changes, and a well-known way for bacteria to monitor and respond to their environment is by the use of two-component signal transduction systems (TCS).

1.2 Two component systems

TCS are typically organized in operons that encode a sensing histidine kinase (HK) and a response regulator (RR). The HK harbors an N-terminal input domain that recognizes a specific stimulus. The information is then transduced through intramolecular conformational changes, resulting in the phosphorylation and activation of the C-terminal transmitter domain. This domain, in turn, activates its cognate receiver, encoded by the N-terminal domain of the RR. Once activated, the RR gives rise to an intracellular response through the C-terminal effector (or output) domain. This response typically results in differential gene expression (Fig. 3), but it can also result in a protein-protein interaction (e.g., chemotaxis) or protein-DNA/RNA interactions leading to differential gene expression. Stimulus perception mechanisms for well-characterized HKs, can be an indication for trying to predict the biological function of uncharacterized TCSs, even if sequence homology is generally a poor predictor of sensing mechanisms or specific stimuli, while domain architecture may provide clues that assist in assigning HKs to one of three groups: extracellular sensing, membrane sensing and cytoplasmic sensing (15, 16).

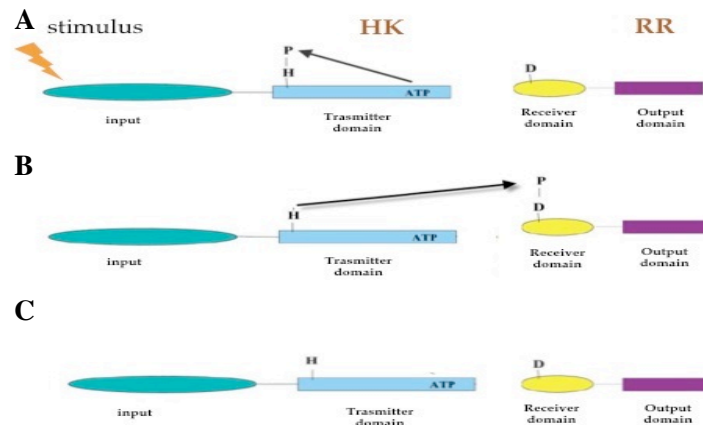


FIG 3 TCS mechanism of action. **(A)** Autophosphorylation of the histidine residue (H) in the transmitter domain of the sensor (sensor activation); **(B)** Transferring of the phosphate group (P) to an aspartic acidic residue in the receiver domain of the RR (receiver activation); **(C)** Dephosphorylation of the RR to set the system back to the prestimulus state (15).

Extracellular sensing HKs typically sense stimuli located in the extracellular space, like solutes or nutrients. Examples are represented by the TCSs EnvZ/OmpR (63) and NtrB/NtrC in *E. coli*. (34). Transmembrane sensing HKs usually respond to membrane associated stimuli such as turgor, mechanical stress, quorum sensing molecules or stimuli derived from membrane-bound enzymes. Classical examples are TCSs such as LiaS/R of *B. subtilis* (24) and the *S. pneumoniae* ComD/E (52). Cytoplasmic TCSs respond to diffusible or internal stimuli, such as O₂ or H₂. They also sense the presence of intracellular solutes or of proteins signaling the metabolic or developmental state of the cell or of the cell cycle (32). Examples are the CheA/Y TCS of proteobacteria (53) and ArcB/A of *E.coli* (31) (Fig. 4).

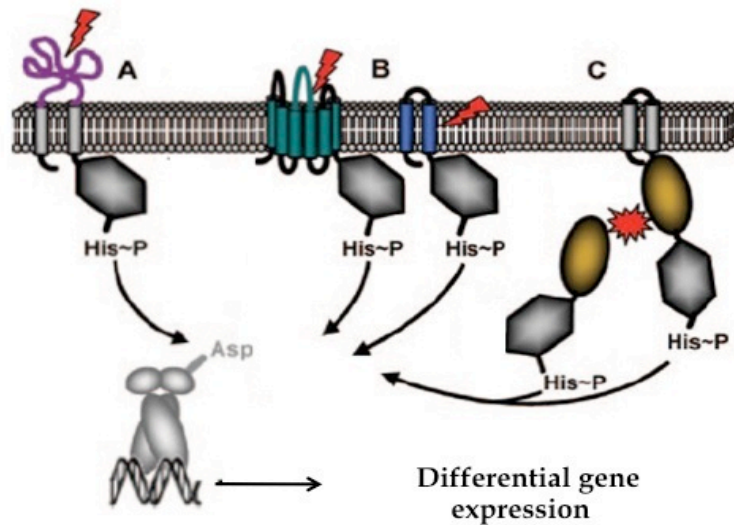


FIG 4 Schematic representation of the three different mechanisms of stimulus perception. (A) Periplasmic-sensing HKs. (B) HKs with sensing mechanisms linked to the transmembrane regions. (C) Cytoplasmic-sensing HKs. The stimulus is represented by a red arrow or red star (16).

1.3 Two component systems in GBS

Overall, the role of TCS in GBS pathogenesis is not well understood and so far, only a few TCS have been already studied in *Streptococcus agalactiae*. In the sequenced NEM316 and 2603 V/R strains, 20 and 17 TCSs have been identified respectively (17, 18). The most studied system is CovRS, an important regulator in *Streptococcus* spp. In GBS, the CovRS regulon extends to 7-27% of the genome (depending on growth conditions), and includes different functional categories, such as cell envelope, cellular processes, metabolism and virulence factors (19-22). Only a few other TCSs have been studied in GBS. The DltS/DltR has been showed to be involved in the

regulation of D-alanyl-LTA biosynthesis (23), a molecule essential for *S. agalactiae* virulence (24). The TCS RgfC/RgfA regulates the expression of bacterial cell surface components (ScpB) and is involved in fibrinogen binding (25, 26). In the TCS CiaH/R, the RR CiaR is involved in intracellular survival within neutrophils, murine macrophages, and human BMEC and it is linked to increased bacterial susceptibility to killing by antimicrobial peptides, lysozyme, and reactive oxygen species (27). Moreover, the Sak189 response regulator was shown to be important in controlling virulence properties *in vivo* as well as the transcription of the β -antigen through the *bac* gene (28). And just recently the two-component response regulator LiaR was shown to regulate expression of genes involved in microbial defence against host antimicrobial systems including genes functioning in cell wall synthesis, pili formation and cell membrane modification. Moreover GBS LiaR mutants are significantly attenuated in mouse models of both sepsis and pneumonia (29).

1.4 Aim of the study and importance

Two component systems have been evolved by bacteria to detect environmental changes and play key roles in pathogenicity. A comprehensive analysis of TCS in GBS has not been previously performed.

In the present study, we aim to better understand the role of TCS in GBS pathophysiology by adopting a step-wise screening strategy. First, inventory, comparative genomics analysis, and sensing mechanism classification were performed through a bioinformatics approach. Second, by transcriptional analysis and identification of

output domains related to virulence, we selected five systems and generated knock-out strains for further study.

In this way we classified 21 TCS and presented evidence for the involvement of two specific TCS in GBS virulence and colonization *in vivo*. Although pinpointing specific TCS stimuli is notoriously difficult, using a combination of techniques we identified two systems with different effects on GBS pathogenesis. For one of the systems, we propose that fructose-6-phosphate, a metabolite in glycolysis, is sufficient to induce a regulatory response involving a sugar transport system.

Our catalogue and classification of TCS not only give an overview of the TCSs distribution in the world of group B *Streptococcus* but also provide new evidences of their importance in the fitness and virulence of GBS.

This work is a precious starting point and it may guide further studies into the role of TCS in GBS pathogenicity and biology.

2. Results

2.1 Identification and comparative genomics of TCS

For the purposes of our study, we focused our main attention on serotype V GBS isolates. Type V is the most common capsular serotype associated with invasive infection in non-pregnant adults and has increased among neonatal invasive disease strains in the recent years, accounting for approximately one-third of clinical isolates in the U.S. population (30). To identify possible TCS, genes predicted to encode HKs or RRs in the GBS type V 2603 V/R genome were collected from the P2CS database (<http://www.p2cs.org>) (31, 32). A total of 38 genes (21 systems) were identified (Table 1). 17 out of these loci contained a cognate pair of HK and RR-encoding genes while an additional 4 TCS genes were orphans. Each TCS locus, whether paired or orphaned, was assigned a number in order of appearance on the chromosome. The predicted TCS proteins were then used as queries to identify corresponding gene loci in 7 other GBS genomes (17, 18, 33). Eight out of 21 TCS were very well conserved (identity>98%) across the genomes. Our analysis was unidirectional, and we do not exclude the presence of additional TCS in the 7 genomes. Thirteen systems had critical polymorphisms in one or more genomes, and the resulting proteins were predicted to be functionally inactive or compromised. However, such variants were especially abundant in draft genomes (pseudochromosomes), and often contained ambiguous nucleotides or contig breaks close to the polymorphism. Therefore, some of the reported polymorphisms may represent sequencing errors, in which case we are underestimating the number of fully functional orthologous systems. TCS-17/RgfAC

presented an interesting case of variability. While TCS-17/RgfAC is complete and conserved in strains CJB111 and COH1 (and O90R), other strains have an orphan TCS-17/RgfAC, where only the RR/RgfA is present. Genomes with an orphan TCS-17 may have undergone recombinatorial events, as they show larger deletions in the locus with short remnants of putative *hk* or *rr* genes. Moreover, RR17/RgfA is less similar (80% identity) than typical (>95%) when comparing the orphaned variants with the paired variants. This suggests a subsequent degeneration of the inactive orphaned locus, or that TCS-17 in strains CJB111, COH1 and O90R could represent a functionally different system.

We also searched the NCBI database of non-redundant protein sequences, and excluded hits in GBS. All our best hits were found in organisms that are phylogenetically close to GBS, and all but two were found in *Streptococcus* spp. Sequence identity varied, and a subset of the TCS may represent a 'Streptococcal set', while systems with the lowest degree of homology may perform functions unique for GBS.

TCS	2603 V/R	Type	Anomalies ^a	CJB111 ^b	Best hit ^c	Id ^d	Ref. ^e
TCS-1	SAG0123	RR		SAM0116	<i>S. uberis</i>	100	
	SAG0124	HK		SAM0117		99	
TCS-2	SAG0182	HK		SAM0183	<i>S. ratti</i>	82	
	SAG0183	RR		SAM0184		78	
TCS-3 (Orphan)	SAG0310	HK	515	SAM0322	<i>S. vestibularis</i>	50	
		-	RR in all strains	SAM0323			
TCS-4	SAG0321	HK		SAM0333	<i>S. iniae</i>	63	<i>liaSR</i> (29)
	SAG0322	RR		SAM0334		85	
TCS-5	SAG0393	RR		SAM0401	<i>S. porcinus</i>	77	
	SAG0394	HK	COHI	SAM0402		67	
TCS-6	SAG0616	RR		SAM0583	<i>E. faecalis</i>	95	<i>sak188/189</i> (28)
	SAG0617	HK	H36B [*] , 18RS21 [*]	SAM0584		78	
TCS-7 (Orphan)	SAG0712	RR	18RS21 [*]	SAM0733	<i>R. albus</i>	54	
		-					
TCS-8	SAG0719	RR		SAM0741	<i>S. infantarius</i>	90	
	SAG0720	HK	H36B	SAM0742		79	
TCS-9	SAG0976	RR		SAM0983	<i>S. criceti</i>	73	
	SAG0977	HK		SAM0984		54	
TCS-10	SAG0984	HK		SAM0991	<i>S. mutans</i>	60	<i>ciaRH</i> (27)
	SAG0985	RR		SAM0992		89	
TCS-11	SAG1016	RR		SAM1027	<i>S. urinalis</i>	49	
	SAG1017	HK	H36B [*]	SAM1028		67	
TCS-12	SAG1327	HK	H36B ^{*/****}	SAM1289	<i>S. gallolyticus</i>	65	
	SAG1328	RR	515 (RR in different locus)	SAM1290		73	
TCS-13	SAG1624	HK	18RS21 [*]	SAM1583	<i>S. ictaluri</i>	51	<i>covRS</i> (21)
	SAG1625	RR		SAM1584		85	
TCS-14	SAG1791	HK		SAM1775	<i>S. infantarius</i>	57	<i>dltRS</i> (23)
	SAG1792	RR	CJB111 ^{*/****} , 515, H36B ^{*/****}	SAM1776		73	

TCS-15 (Orphan)	SAG1922	RR		SAM1860	<i>S. pneumoniae</i>	64
TCS-16	SAG1946	RR		SAM1885	<i>S. canis</i>	77
	SAG1947	HK		SAM1886		
TCS-17 (Orphan)			HK in COH1,CJB111	SAM1896	<i>S. pneumoniae</i>	<i>rgfAC</i> (25)
	SAG1957	RR	COH1 ^{**} , CJB111 ^{**} , A909 ^{***} , H36B	SAM1897		
TCS-18	SAG1960	HK	18RS21	SAM1900	<i>S. bovis</i>	58
	SAG1961	RR		SAM1901		
TCS-19	SAG2054	RR	COH1	SAM1962	<i>S.</i> <i>pseudoporcinus</i>	59
	SAG2055	HK		SAM1963		
TCS-20	SAG2122	RR		SAM2038	<i>S. ratti</i>	65
	SAG2123	HK		SAM2039		
TCS-21	SAG2127	HK	18RS21	SAM2043	<i>S. porcinus</i>	70
	SAG2128	RR	18RS21 (Absent)	SAM2044		

TABLE 1 Comparative genomics of TCS

^aStrains/genomes in which orthologous HK or RR proteins were predicted to be inactivated or exhibited other variations compared to the 2603 V/R strain. Genomes analyzed were A909, 515, H36B, 18rs21, NEM316, COH1 and CJB111; ^bNon-GBS species in which the most similar TCS was identified (combined best score for HK and RR proteins, respectively); ^cPercent amino acid identity of HK and RR with the most similar non-GBS putative orthologues. Query cover >95%; ^dTIGR gene names of *hk* and *rr* genes in the CJB111 strain used in the experimental studies; ^ePreviously reported name (citation); *Reduced sequence quality, **Sequence identity <90%, ***Minor truncation (<40 aa).

2.2 Domain architecture for TCS in the genome of CJB111

For further experimental analysis we shifted our focus to the serotype V strain CJB111 that is more virulent than 2603 V/R in mouse models, and for which a custom microarray was available in-house. The CJB111 TCS gene identified are listed in Table 1. We analyzed the domain architecture of all the HK proteins in the genome of CJB111 and predicted the mechanism of stimulus perception according to criteria reported in the literature (16) (Fig. 5). Nine of the HKs contained an N-terminal domain with two transmembrane helices with a spacer of 50-300 aa, typical for extracellular (EX) sensing. Eight HKs contained 2-6 predicted transmembrane-spanning regions separated by short spacers, and were predicted to be membrane sensing (TM). Only one HK was classified as cytoplasmic (C) sensing.

We also observed that all the RR proteins had a DNA-binding output domain, indicating a role as direct transcriptional regulators. Interestingly, the LytTR output domain was the second most common output domain in GBS (15%), while it accounts for a smaller percentage (4%) in prokaryotes in general. LytTR-type output domains have been noted for the control of virulence factors in several important bacterial pathogens (32).

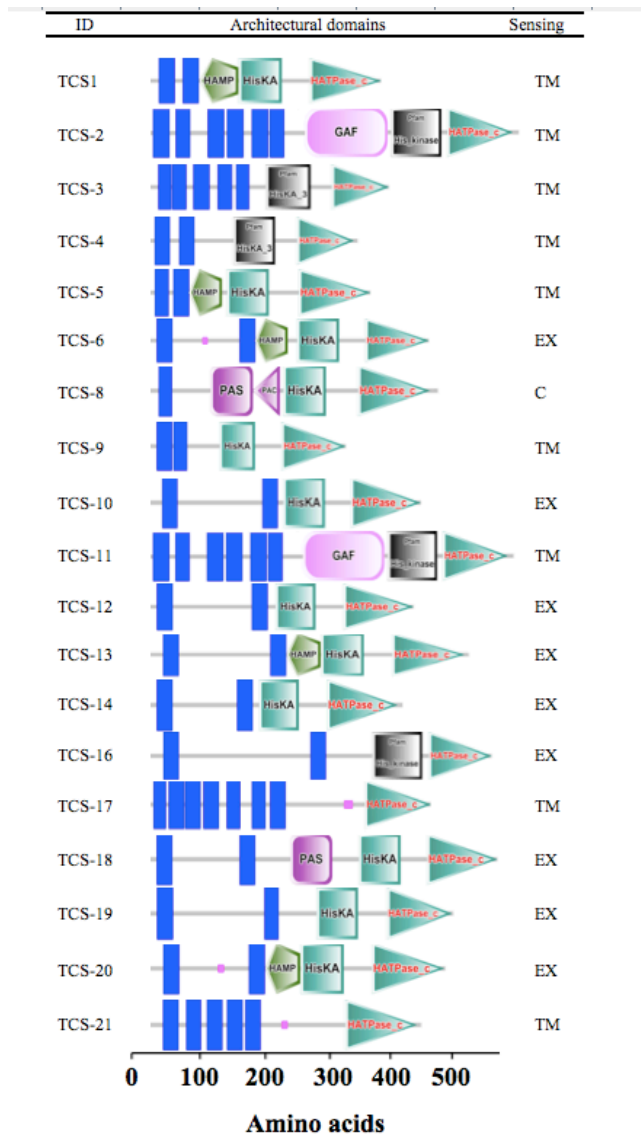


FIG 5 Domain architecture of histidine kinases. Protein sequences were analyzed using SMART <http://smart.embl-heidelberg.de> and PFAM domains were included. The scale bar shows the length of sequences in amino acids. Blue vertical bars represent putative transmembrane helices and pink squares represent low complexity regions. Various functional domains are indicated by the remaining colored elements and using the SMART nomenclature (e.g. GAF, PAS, HAMP, PAC). The SMART HATPasec domain in TCS-17/RgfAC is an outlier homolog and was found using the schnipsel database. Sensing mechanisms were manually predicted as TM (TransMembrane), EX (Extracellular) and C (Cytoplasmic).

2.3 Transcriptional analysis of TCS

Transcriptional analysis was performed in early logarithmic (EL) and early stationary (ES) phase using a custom microarray chip designed on the CJB111 genome. We noted that several TCS were significantly up-regulated in ES phase, and 3 of these (TCS-2, TCS-16, TCS-21) were up-regulated 4- fold or more (data not shown). As many TCS respond to stress conditions such as those encountered in stationary phase (lack of nutrients, low pH, and accumulation of toxic metabolites), we hypothesized that these systems could be involved in bacterial stress responses and selected them as targets for mutagenesis. To further understand the levels of expression of each selected TCS during bacterial growth *in vitro*, we measured the gene transcripts of the HKs at four time points (representing early, mid-,

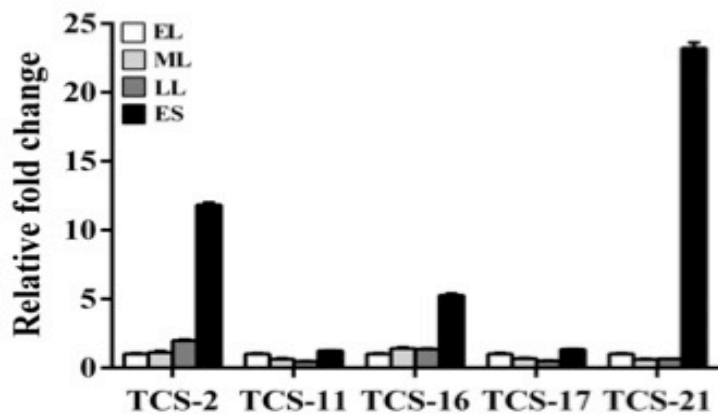


FIG 6 qRT-PCR analysis of selected TCS in four different phases of growth: early (EL), mid (ML), and late logarithmic (LL), and early stationary phase (ES). Each column represents three biological replicates, and error bars show the SEM. Fold change is relative to the expression level of each system in EL phase.

TCS	Name	Type	Fold change ^a	<i>p</i> -value ^b
	SAM0183	HK	6.1	7.4x10 ⁻⁴
TCS-2	SAM0184	RR*	5.6	6.0x10 ⁻³
	SAM1027	RR*	0.9	n.s.
TCS -11	SAM1028	HK	1.5	n.s.
	SAM1885	RR	4.5	3.8x10 ⁻³
TCS -16	SAM1886	HK	5.5	1.1x10 ⁻³
	SAM1896	HK	1.1	n.s.
TCS -17	SAM1897	RR*	1.6	n.s.
	SAM2043	HK	37.0	6.0x10 ⁻⁸
TCS -21	SAM2044	RR	19.5	6.3x10 ⁻⁵

Table 2 CJB111 expression of selected TCS (a)Relative expression of the TCS in ES compared to EL growth phase; (b)The fold change was considered not significant (n.s.) if $p > 0.05$; *Contains a LytTR output domain.

and late logarithmic and early stationary phases) using a qRT-PCR analysis (Fig. 6). These data confirmed that TCS-2, TCS-16, and TCS-21 are up-regulated only in ES phase.

Transcriptional regulators with the LytTR-type output domains control production of virulence factors in several important bacterial pathogens (32). We consequently selected the three TCS containing RR with a LytTR-type DNA binding domain, i.e TCS-2 (up-regulated at ES phase), TCS-11 and TCS-17/RgfAC, as mutagenesis targets. Thus, a total of five TCS exhibiting either the presence of a LytTR domain and/or up-regulation during ES were selected for further experimentation (Table 2).

2.4 Expression microarray analysis of TCS mutants

The 5 selected TCS loci were modified genetically by in-frame deletion of the genes encoding RRs. There were no apparent differences in colony size, hemolysis, or other macroscopic features between the wild-type strain and the five isogenic mutant strains on blood agar or tryptic soy agar plates (data not shown). Mutant strains grown in complex medium exhibited growth curves identical to the wild-type parental strain (Fig. 7). Global transcriptional analysis was performed by microarray technology. Gene expression of all the predicted genes (n=2,232) in the CJB111 genome was performed by comparing the WT strain with each of the 5 mutant strains in ES phase (Fig. 8A). Experimental design, chip validation, quality control and data analysis were performed as described (see Materials and Methods).

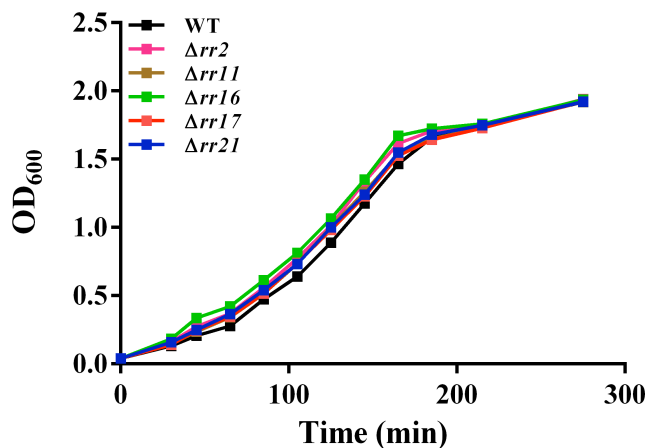


FIG 7 Growth curves of WT and isogenic mutant strains in THB medium. Curves represent the mean of triplicate samples.

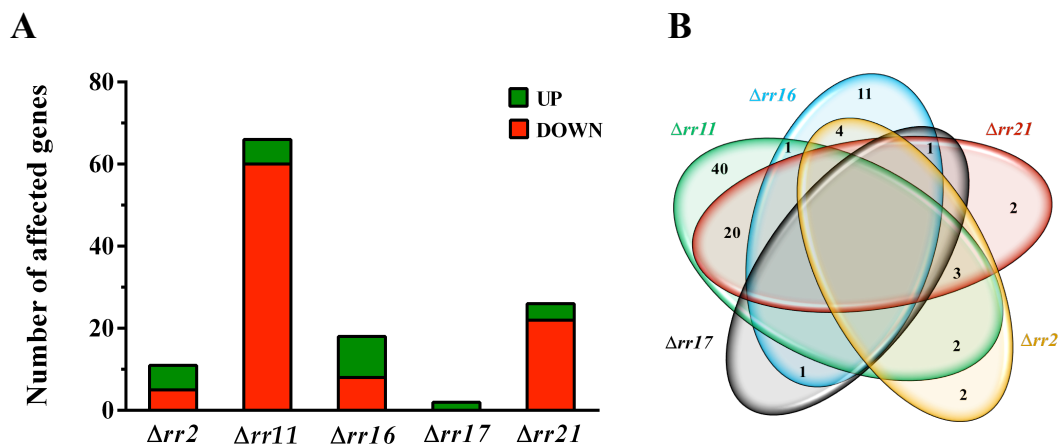


FIG 8 Microarray analysis of TCS mutant strains. Columns represent the number of up- (green) or down-regulated (red) genes in early stationary (ES) phase, compared to the WT strain. Threshold used is ± 2 -fold change and $p \leq 0.05$ (A). Venn Diagram showing overlap of gene regulation between the mutants (B).

Further validation of the microarray data was performed by qRT-PCR using probes for 9 independent transcriptional units (Fig. 9). Overall, all five mutants exhibited differentially transcribed genes compared to the wild type when using a permissive threshold (\pm 2-fold change and $p < 0.05$). The number of regulated genes ranged from 2 ($\Delta rr17$) to 66 ($\Delta rr11$). Two mutants ($\Delta rr11$ and $\Delta rr21$) showed predominantly down-regulated genes, suggesting that these RRs act as activators. We observed that some genes appeared regulated in two or more independent mutant strains (Fig. 8B). In particular, 20 genes were regulated in both $\Delta rr21$ and $\Delta rr11$ (19 genes down-regulated and 1 gene up-regulated in both strains). A more stringent threshold was applied to identify the most highly regulated genes (\pm 4-fold change and $p < 0.05$). Three mutants ($\Delta rr2$, $\Delta rr11$ and $\Delta rr16$) showed a total of 18 highly regulated genes and in two of them such genes were identified adjacent to the TCS locus (Table 3). In particular, the mutant $\Delta rr2$ exhibited down-regulation of SAM0185 and SAM0186, encoding two proteins similar to LrgAB in *Streptococcus mutans*. In this species LrgAB is reported to be under the control of an adjacent TCS (homologous to TCS-2) and was suggested to have a role in the control of virulence and biofilm formation (34, 35). The mutant $\Delta rr16$ showed strong down-regulation of an adjacent phosphotransferase system (PTS), and concomitant up-regulation of another PTS system in a different locus. All the highly regulated genes were subjected to confirmation by qRT-PCR, using one probe set per transcriptional unit (Table 3). Moreover, qRT-PCR experiments were repeated on chromosomally complemented

strains where the deleted *rr* gene was replaced with the WT form, which confirmed that the WT phenotype was restored (Table 3).

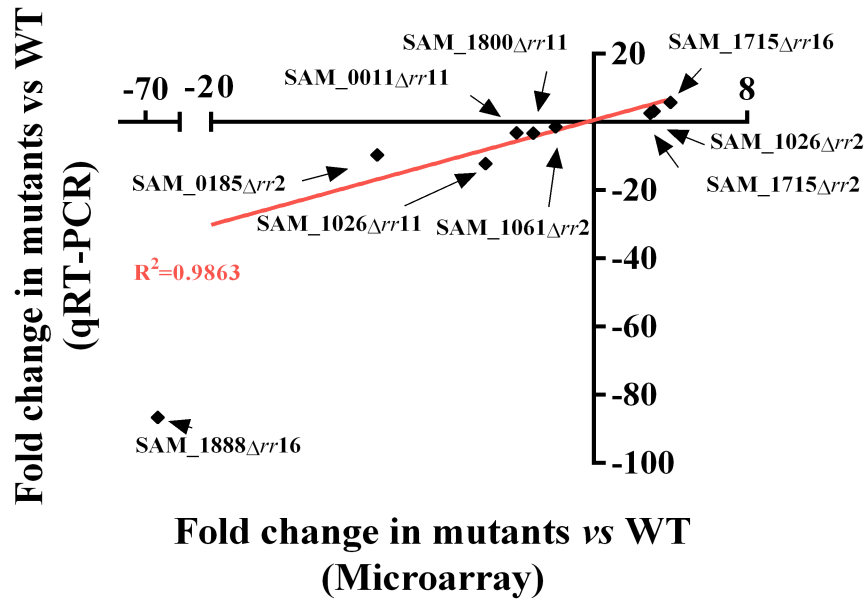


FIG 9 Correlation between microarray and qRT-PCR. Values obtained for the two methods were plotted on the *x* and *y* axes. Each dot represents the fold change of mutant versus WT for a highly regulated gene indicated with an arrow. The mutant strains used were $\Delta rr2$ (red), $\Delta rr11$ (green) and $\Delta rr16$ (blue).

Mutant	Name	Annotation	Gene	Fold change microarray	<i>p</i> -value ^a	Fold change qRT-PCR ^b
<i>Δrr2</i>	SAM0185	LrgA family subfamily, putative	<i>lrgA</i>	-11.5	4.0x10 ⁻⁵	-6.14/-1.18
	SAM0186	LrgB family protein	<i>lrgB</i>	-8.8	1.2x10 ⁻⁴	
<i>Δrr11</i>	SAM0011	Phosphoribosylformyl- glycinamide synthase		-4.0	2.2x10 ⁻⁴	
	SAM0012	Amidophosphoribosyl- transferase	<i>purF</i>	-4.0	3.0x10 ⁻³	-2.23/+2.98
	SAM0013	Phosphoribosylformyl- glycinamide cyclo-ligase	<i>purM</i>	-4.3	2.4x10 ⁻⁴	
	SAM0014	Phosphoribosylglycyl- amide formyltransferase	<i>purN</i>	-4.3	1.8x10 ⁻³	
	SAM0064	Ribosomal protein S5	<i>rpsE</i>	-4.4	1.8x10 ⁻⁵	-2.01/+1.56
	SAM1026	Carbon starvation protein, putative	<i>cstA</i>	-5.7	1.6x10 ⁻⁵	-10.95/+2.11
	SAM1057	Conserved hypothetical protein		-5.1	1.8x10 ⁻⁵	
	SAM1058	Conserved hypothetical protein		-5.2	5.8x10 ⁻⁵	
	SAM1059	Carbamoyl- phosphate synthase, large subunit	<i>carB</i>	-7.4	3.0x10 ⁻⁷	-4.72/-1.69
	SAM1060	Carbamoyl- phosphate synthase, small subunit	<i>carA</i>	-4.2	4.2x10 ⁻²	
<i>Δrr16</i>	SAM1715	PTS system, IIC component	<i>fruA-2</i>	+4.0	1.4x10 ⁻⁴	+3.25/-1.06
	SAM1716	PTS system, IIA component	<i>fruA-2</i>	+4.1	2.6x10 ⁻⁴	
	SAM1887	PTS system, IID component		-31.6	1.6x10 ⁻⁷	-324.0/+1.72
	SAM1888	PTS system, IIC component		-72.0	1.0x10 ⁻⁷	
	SAM1889	PTS system, IIB component		-55.7	1.0x10 ⁻⁶	-6.14/-1.18

SAM1890	PTS system, IIA component, putative	-52.0	1.8×10^{-7}
---------	--	-------	----------------------

TABLE 3 Highly regulated genes in early stationary phase. (a) Inclusion threshold is $p \leq 0.05$ and fold change ± 4 (compared to WT strain). (b) Fold change of knockout/complemented strains compared to the WT strain.

2.5 Phenotype microarray screening shows that TCS-16 influences carbon source utilization

Our microarray analysis showed differential regulation of two different PTS (SAM1715-1716 and SAM1887-1890) in the $\Delta rr16$ mutant strain, suggesting a possible involvement in the monitoring of carbon source availability. The WT and $\Delta rr16$ strains were grown on 192 different single carbon sources using the phenotype microarray technology (Fig. 10). One compound showed a clear difference between the WT and mutant strain. The WT strain exhibited growth comparable to the positive control when supplied with fructose-6-phosphate (Fru-6-P), while the $\Delta rr16$ strain showed no growth. The experiment was repeated using the complemented strain $KIrr16$, showing a growth profile indistinguishable from the WT strain (Fig. 10).

To confirm this phenotype in an independent system, and to understand if it could be extended to other hexose-6-phosphate sugars, we used a chemically defined medium (36) where glucose, fructose, mannose, or their corresponding hexose-6-phosphate counter parts were used as the primary carbon source (Fig. 11). The WT, $\Delta rr16$ and $KIrr16$ strains grew well on glucose, fructose and mannose while only the WT and $KIrr16$ strains grew on Fru-6-P. The other phospho-sugars did not allow any bacterial growth. We concluded that TCS-16 is necessary for growth of strain CJB111 on Fru-6-P as the primary carbon source.

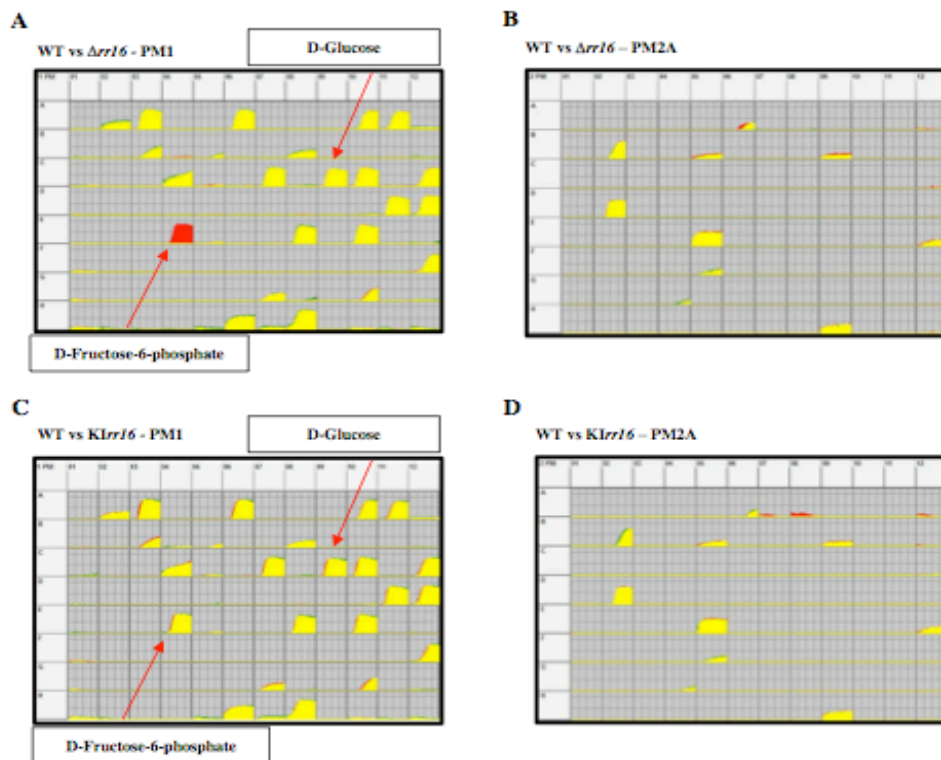


FIG 10 Phenotype microarray analysis on WT, $\Delta rrl6$ and $Klrr16$ was performed using PM1 and PM2A plates (<http://www.biolog.com/pdf/pmlit/PM1-PM10.pdf>). Kinetic plots are shown in red (WT) or in green (mutant and complemented strains), and superimposition is shown in yellow. Metabolic differences between WT and $\Delta rrl6$ or WT and $Klrr16$ mutant are shown in superimposed kinetic plots obtained by growing bacteria on PM1 (A and C) or PM2A (B and D).

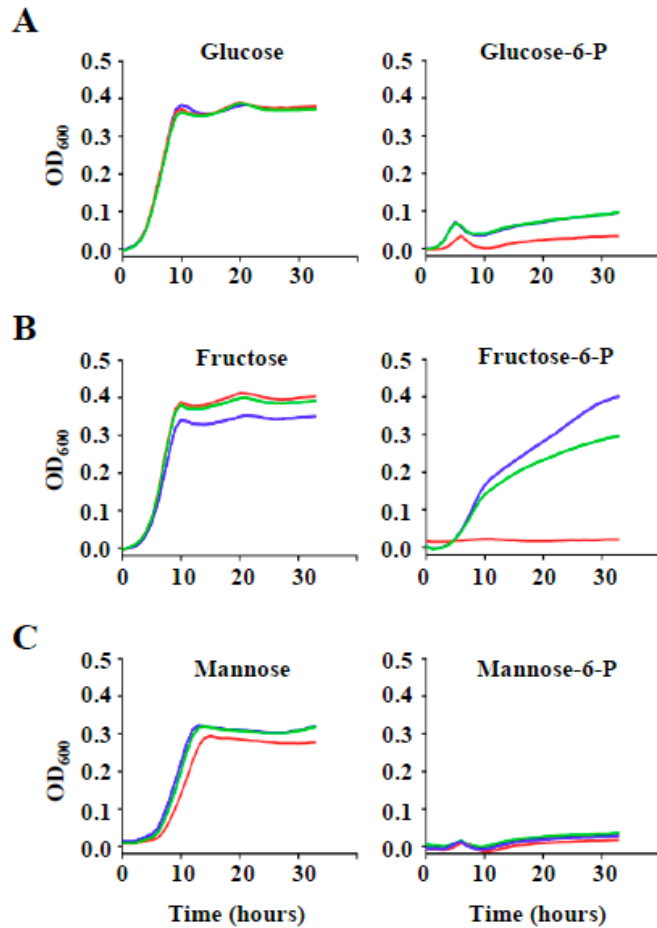


FIG 11 Growth curves of WT (blue), $\Delta rr16$ (red) and $Krr16$ (green) in CDM supplemented with 10 mg/ml of glucose (left) or glucose-6-P (right) (**A**), fructose (left) or fructose-6-P (right) (**B**), mannose (left) or mannose-6-P (right) (**C**). Growth curves are from triplicate samples, and background (negative control, no sugar added) was subtracted.

2.6 TCS-16 gene regulation in response to extracellular Fru-6-P

We subsequently investigated the impact of Fru-6-P on transcription of TCS-16 and its adjacent PTS system by qRT-PCR. Bacteria grown in CDM were subjected to a substitution of glucose for Fru-6-P upon entry in mid-logarithmic phase (see materials and methods). The *hkl6* gene transcription increased 22-fold when bacteria are exposed to Fru-6-P compared to glucose (Fig. 12A). This response was observed in the WT, absent in $\Delta rr16$, and partially restored in the complemented $KIrr16$ strain. Concomitantly (Fig. 12BC), a similar pattern was observed for the adjacent PTS system (3,000-fold up-regulation) and for SAM1402 (2.5-fold up-regulation), a putative hexose-6-P transporter that we identified in the genome of CJB111. A down-regulation of *sam1402* gene (1.5-fold) in the $\Delta rr16$ strain was also observed in the microarray. Fru-6-P is an intracellular metabolic intermediary of the glycolytic pathway. Bacterial lysis constitutes a possible scenario where Fru-6-P would be found in the extracellular space. We wanted to investigate if TCS16 would respond under such conditions. Bacteria were grown in CDM until mid-logarithmic phase, and the medium was changed to CDM without glucose in the presence or absence of bacterial lysate (see materials and methods). The transcriptional levels of TCS-16, of its adjacent PTS system and of the putative hexose-6-P transporter were then analysed by qRT-PCR. The *hkl6* gene transcription increased 10-fold when bacteria were exposed to bacterial lysate compared to the control (Fig. 12D). Concomitantly, an up-regulation of the PTS system (200-fold) and *sam1402* gene (5-fold) was

observed (Fig. 12E-F). These responses were absent in $\Delta rr16$, and totally restored in the complemented $KIrr16$ strain.

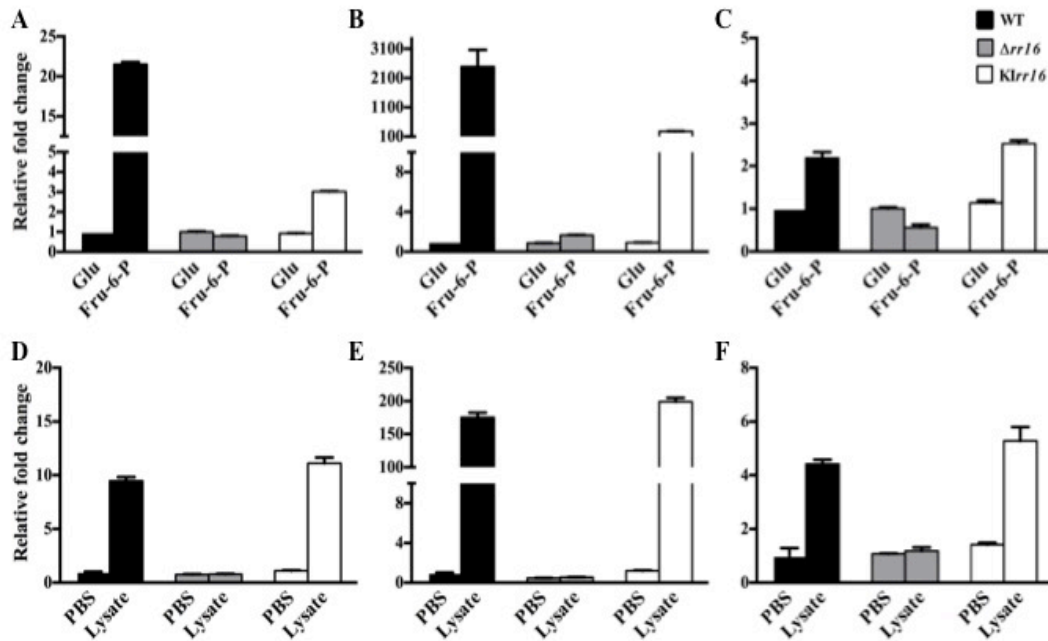


FIG 12 qRT-PCR with probes for SAM1885 (HK) (**A**, **D**), SAM1888 (PTS, IIC component) (**B**, **E**), and SAM1402 (putative hexose-phosphate transporter) (**C**, **F**), using RNA extracted from WT (black), $\Delta rr16$ (gray) and $KIrr16$ (white). In the top panel (**A-C**), bacteria grown in CDM were subjected to a pulse of either glucose (Glu) or fructose-6-P (Fru-6-P) as the main carbon source for 30 min prior to RNA extraction. Columns represent relative gene expression when exposed to Fru-6-P, compared to when grown in glucose. In the bottom panel (**D-F**), bacteria grown in CDM were subjected to a pulse of PBS or bacterial lysate for 30 min prior to RNA extraction. Columns represent relative gene expression when exposed to bacterial lysate, compared to the PBS control. The experiment was performed twice. Columns represent technical triplicates, and error bars show the SEM.

2.7 The RR16 recombinant protein is insoluble when expressed in *E. coli*

To test if the PTS system and the putative hexose-phosphate transporter were direct targets of the RR16 protein, we decided to perform an electrophoretic mobility shift assay (EMSA). For this purpose the recombinant RR16 protein (rRR16) was expressed in *E. coli* with a His-tag and purified using the classical affinity chromatography approach. We tested different temperatures (37-25°C), different induction times (2-6-8 hours), different *E. coli* strains (BL21 DE3, T7 express), different growth media (LB, Biosilta, HTMC) and different lysis conditions (mechanical and chemical) and we set up the best conditions to obtain a soluble rRR16 protein. *E. coli* T-7 express cells transformed with pET15TEV-rRR16-His plasmid were grown in the Biosilta medium at 30°C and induced for 2 hours at 25°C. Cells were then chemically lysed and 20% of the rRR16-His protein (33 KDa) was found in the soluble fraction (Fig. 13A).

The rRR16-His was then purified from the soluble fraction using a His-tag affinity purification strategy (Fig. 13B). Eluted fractions were then pooled, concentrated up to 1/6 of the initial volume and quantified using the BCA method. Samples showed a final concentration of 0.6 µg/µl but a high number of contaminant proteins were also detected on the Coomassie gel. The rRR16-His protein seemed to represent only the 20% of the total proteins in the sample (Fig. 13C). The concentration obtained was then too low to be used for an EMSA.

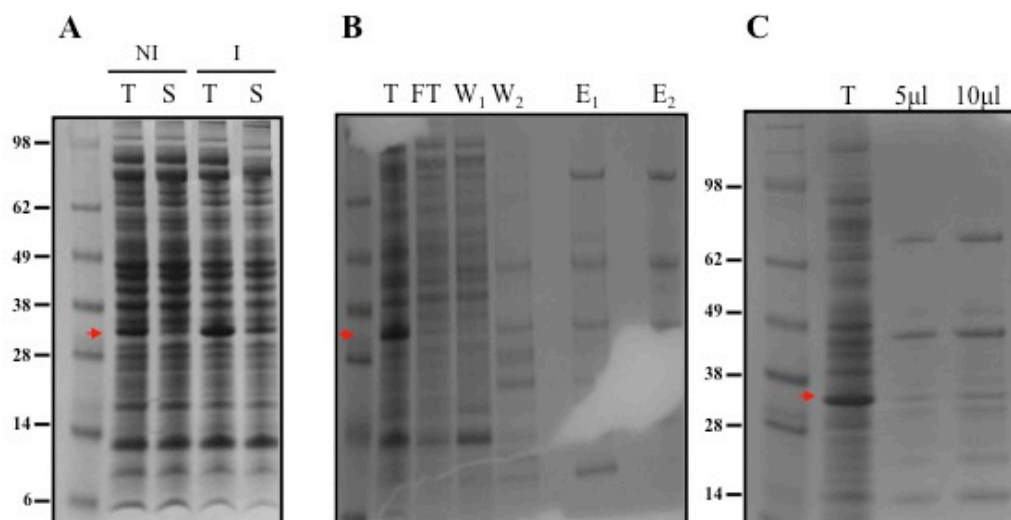


Figure 13 Expression and purification of the rRR16-His protein. *E. coli* T-7 express cells expressing rRR16-His protein were lysate before (NI) and after (I) IPTG induction. Fraction representing the total lysate (T) and the soluble part are displayed on an SDS/PAGE gel and stained with Coomassie blue (**A**). The elution profiles of rRR16-His protein from a Ni²⁺ column. Purification was performed only on the soluble fraction obtained after induction. T, the total extract; FT, flow-through fraction; W₁₋₂, wash fractions; E₁₋₂, fractions eluted with imidazole. Fractions are displayed on an SDS/PAGE gel and stained with Coomassie blue (**B**). Protein profile in the elution fractions after Amicon concentration. T, total extract; lane 3-4 show different amount of the same sample (**C**). The red arrow shows the 33 KDa rRR16-His protein.

To improve the purification protocol we needed to obtain more soluble protein. For this reason we decided to express the rRR16 protein fused with the His-tag and also with a solubility carrier, the MBP (maltose binding protein).

E. coli BL21-DE3 cells transformed with pMal-rRR16-MBP-His plasmid were grown in the Biosilta medium at 30°C and induced for 8 hours at 25°C. Cells were then chemically lysed and almost 90% of the rRR16-MBP-His protein (70 KDa) was found in the soluble fraction (Fig. 14A).

Using a His-tag affinity purification strategy the 50% of the rRR16-MBP-His protein was purified from the soluble fraction and treated with the TEV protease to remove the carrier protein (Fig. 14B). Unexpectedly, only 10% of the rRR16-MBP-His was successfully cleaved by the TEV, suggesting that the cleaving link was not well accessible for the protease (Fig. 14C).

To then examine the presence of aggregates (or micelles), the samples obtained after the His-tag purification were loaded on a size exclusion chromatography column (SEC). As showed in Fig. 14DE two fractions were obtained. The first one (Fig. 14D) was obtained at a retention time typical of 400 KDa proteins. We then hypothesized that in this fraction were present aggregates of rRR16-MBP-His proteins, as the main band on the SDS gel is a 70 KDa protein. The second one, obtained at a retention time typical of 40 KDa proteins, contained the MBP (arrow1 Fig. 14E) and two unknown smaller proteins (arrow 2-3 Fig. 14E).

MS analysis was unsuccessful and for some reason we were not able to identify the unknown proteins. In any case also this second purification approach did not allow us to obtain a good amount of soluble rRR16 protein.

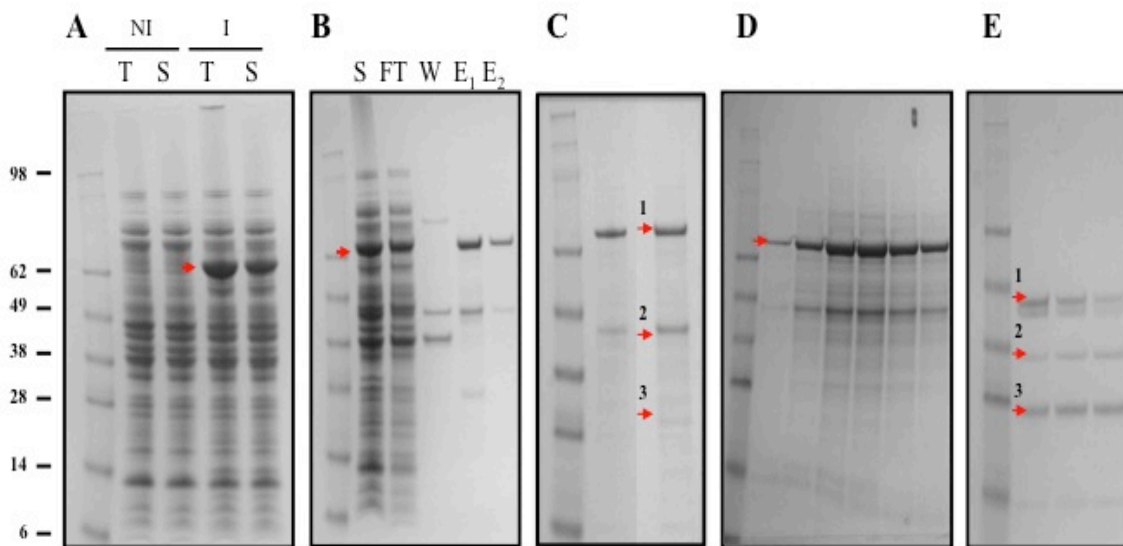


Figure 14 Expression and purification of the rRR16-MBP-His protein. SDS/PAGE gel and stained with Coomassie blue *E. coli* BL21 DE3 cells expressing rRR16-MBP-His protein were lysate before (NI) and after (I) IPTG induction. Fraction representing the total lysate (T) and the soluble part are displayed. The red arrow shows the rRR16-MBP-His protein (A). The elution profiles of rRR16-His protein from a Ni^{2+} column. Purification was performed only on the soluble fraction obtained after induction. S, soluble part; FT, flow-through fraction; W, wash fraction; E_{1-2} , fractions eluted with imidazole. The red arrow shows the rRR16-MBP-His protein (B). Protein profile of the E_1 fraction before (lane 2) and after (lane 3) TEV treatment. Arrow1, rRR16-MBP-His; arrow 2, MBP-His; arrow 3 rRR16 (C). The elution profiles of rRR16-His protein from a SEC column obtained with 130 ml of elution volume. Red arrows shows the rRR16-MBP-His protein (D). The elution profiles of rRR16-His protein from a SEC column obtained with 200 ml of elution volume. Arrow1, MBP; arrow 2-3, unknown proteins analyzed using MS (E).

2.8 TCS-16 influences vaginal persistence in mice

In a recent work, carbon catabolite repression in *S. pyogenes* was shown to influence asymptomatic colonization of the murine vaginal mucosa, suggesting that availability of carbon sources may be subject to monitoring by the bacteria (37). We subsequently investigated whether TCS16 could play a role in bacterial survival during colonization, and utilized the $\Delta rr16$ mutant strain in a mouse model of GBS vaginal colonization (38, 39). CD-1 mice in estrus were inoculated with $\sim 1 \times 10^7$ CFU in the vaginal lumen and, on successive days, bacteria were recovered by swabbing and quantified by serial dilution and plating on selective media. Interestingly, the $\Delta rr16$ mutant exhibited decreased persistence in the vaginal tract (Fig. 15A). The statistically significant differences were observed at later time points during the experiment ($p=0.004$, day 5; $p=0.02$, day 7), and suggested a gradual decline in colonization with the mutant strain while the WT remained relatively stable throughout the experiment. Identical experiments were performed with the remaining mutant strains, and results were similar to those of the WT strain, underlining that the phenotype seen in the $\Delta rr16$ mutant was unique among the strains tested.

The phenotype observed above may be due to reduced fitness at the vaginal mucosa and/or reduced adhesion. To test the latter, we investigated bacterial adhesion to vaginal epithelial cells, using a previously described method (39, 40). Bacteria were incubated with confluent HVEC for 30 min, washed extensively, and following cell lysis the bacteria were enumerated. No differences were observed between the WT and $\Delta rr16$ strains (Fig. 15B).

In order to test our alternative hypothesis, we attempted to at least partly mimic the ecological niche. Vaginal lavages were collected from CD-1 mice and inoculated

with $\sim 1 \times 10^6$ CFU of WT or $\Delta rr16$ strains. Bacterial growth *in vitro* was followed by viable counts, and after 26 hours a statistically significant ($p=0.028$) difference was observed (Fig. 15C). The results suggested that $\Delta rr16$ exhibited impaired growth/survival compared to the WT strain. In a parallel control experiment, bacteria were incubated in PBS without any vaginal mucoid components (Fig. 15D). Both WT and mutant strains showed a rapid decline in viable counts and after 26 h the vast majority (>99.9%) of bacteria were no longer viable. This clearly showed that the limited presence of vaginal mucoid components was necessary to sustain survival and/or growth of the bacteria during the course of the experiment.

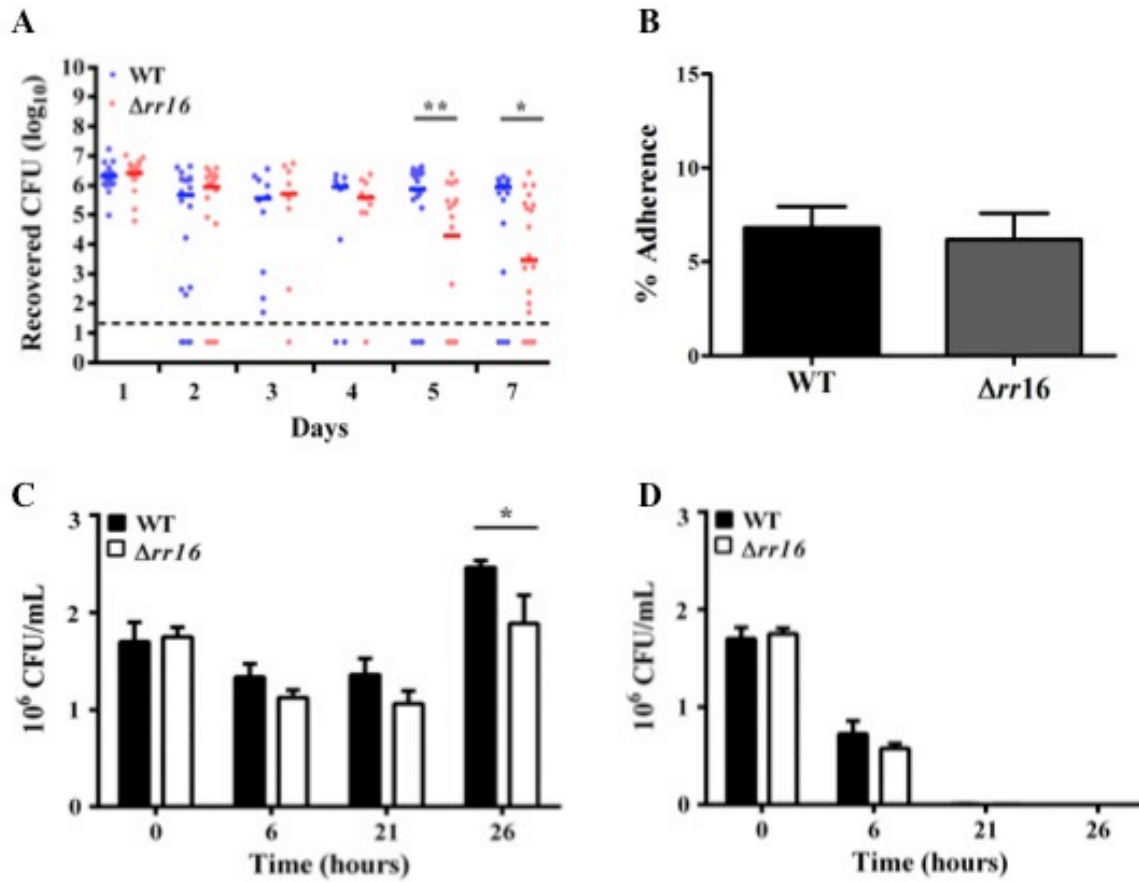


FIG 15 Murine vaginal colonization model. The vaginal lumen of CD-1 mice was inoculated with 10^7 CFU of WT or $\Delta rr16$ bacteria and bacterial persistence was followed by viable counts. Results shown are from two independent experiments. The detection limit is represented by a dashed line. Horizontal bars represent medians, and the Mann-Whitney U test was used for statistical analysis (**A**). Adherence to HVEC cells by WT and $\Delta rr16$ strains. Data are expressed as the total adherent CFU recovered compared to the input inoculum (MOI of 1; $\sim 1 \times 10^5$ CFU) (**B**). *In vitro* growth of WT and $\Delta rr16$ strains in PBS containing vaginal fluid (**C**) or in PBS (**D**). Triplicate samples were used and error bars show the SEM. Statistical analysis was performed by 2-way ANOVA.

2.9 TCS-17/RgfAC influences virulence in a murine model of systemic infection

To further investigate the role of the selected TCS in GBS pathogenesis, we compared the relative virulence of CJB111 with the Δrr mutants using an *in vivo* mouse model of infection (40, 41). CD-1 mice were infected intravenously with 1.5×10^7 CFU of the WT or mutant strains. Bacteremia was confirmed in all mice by viable counts on blood samples collected 24 h post-infection, and there was no significant difference in bacterial loads between WT and mutant strains (data not shown). Over the course of infection, animals were sacrificed at individual end-points (when moribund) or upon termination of the experiments, and blood, brain and lung tissues were collected for bacterial counts. Overall, the only mutant strain with a virulence phenotype was $\Delta rr17$, which exhibited a significantly higher mortality compared to that observed during infection with the WT strain ($p=0.003$, Log Rank test) (Fig. 16A). Interestingly, no significant differences in bacterial loads were observed in brain, blood and lung tissues when comparing the WT and $\Delta rr17$ strain (Fig. 16B-D). Blood and brain tissues from mice infected with the $\Delta rr17$ strain contained more individual samples with very high bacterial counts, but such samples were exclusively from moribund mice (Fig. 16BC). None of the other mutant strains showed an appreciable difference compared to the WT strain (data not shown).

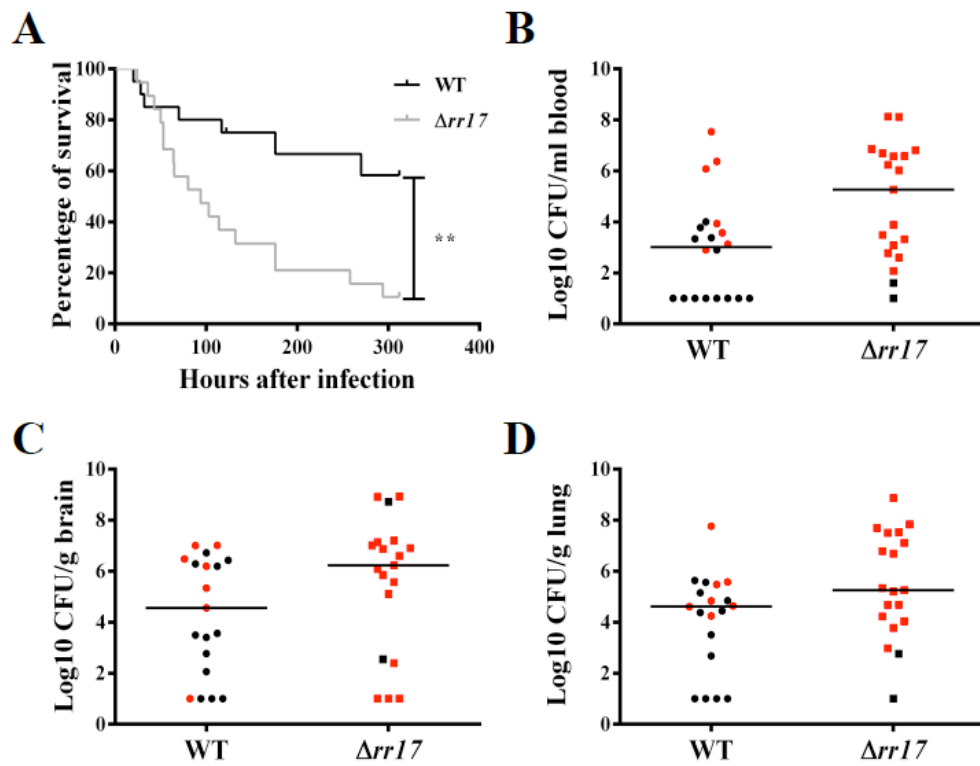


FIG 16 Murine intravenous challenge model. Kaplan-Meier survival plot of mice infected with 1.5×10^7 CFU of bacteria (**A**). The Log-rank test was used for statistical analysis. Bacterial counts (CFU) in blood (**B**), brain (**C**), and lung tissue (**D**) from individual mice. Horizontal bars represent medians. Mice were euthanized when moribund (red) or at the endpoint (black).

2.10 TCS-17/RgfAC shows higher duplication rate in human blood

Our *in vivo* data showed no differences in the ability of WT and $\Delta rr17$ strains to invade the blood brain barrier (Fig.16C). This observation was also confirmed *in vitro*, using a previously described method (40). Bacteria were incubated with confluent hBMEC for 30 min (adherence) or for 2 hours (invasion), washed extensively, and following cell lysis the bacteria were enumerated. For the invasion experiment, bacteria and cells were incubated for other 2 hours with antibiotic before the cell lysis. As expected, no differences were observed between the WT and $\Delta rr17$ strains (Fig. 17A).

Our *in vivo* data showed that the $\Delta rr17$ strain is more virulent then the WT strain in a systemic model of infection. Moreover a higher number of CFU was detected in the blood of mice infected with the $\Delta rr17$ strains compared with those infected with the WT (Fig. 16B). Even if this difference was not statistically significant. To further investigate this phenotype, we compared WT and $\Delta rr17$ strains for their ability to grow in human blood *in vitro*.

Human blood was freshly collected and inoculated with $\sim 1 \times 10^7$ CFU of WT, $\Delta rr17$ or $\Delta Irr17$ strains. Bacterial growth *in vitro* was followed by viable counts, and after 300 minutes a statistically significant difference was observed between WT and $\Delta rr17$ (Fig. 17B). In this condition, the $\Delta rr17$ strain showed a higher number of CFU then the WT and complemented strains suggesting a role for this TCS in bacterial duplication in blood. As after 300 minutes most of the blood cells should be dead, we wondering if the same difference could be observed at earlier time point in human plasma.

For this experiment human blood was freshly collected and then fractionating by centrifugation to separate the plasma. Plasma was later inoculated with $\sim 1 \times 10^7$ CFU of WT and $\Delta rr17$ and bacterial growth *in vitro* was followed by viable counts. After 60 and 180 minutes of incubation in plasma a significant difference in the duplication ability of $\Delta rr17$ strain was observed (Fig. 17C).

Taken together these data suggest that the higher duplication rate of the mutant strain in human blood could not be due to its ability to better escape the immune system. In fact the $\Delta rr17$ strain seems to have an advantage in its duplication rate only when the blood cells are mostly dead or totally absent.

Data shown are preliminary as they are representative of one single experiment. To confirm our hypothesis experiments should be repeated at least other two times with two different donors.

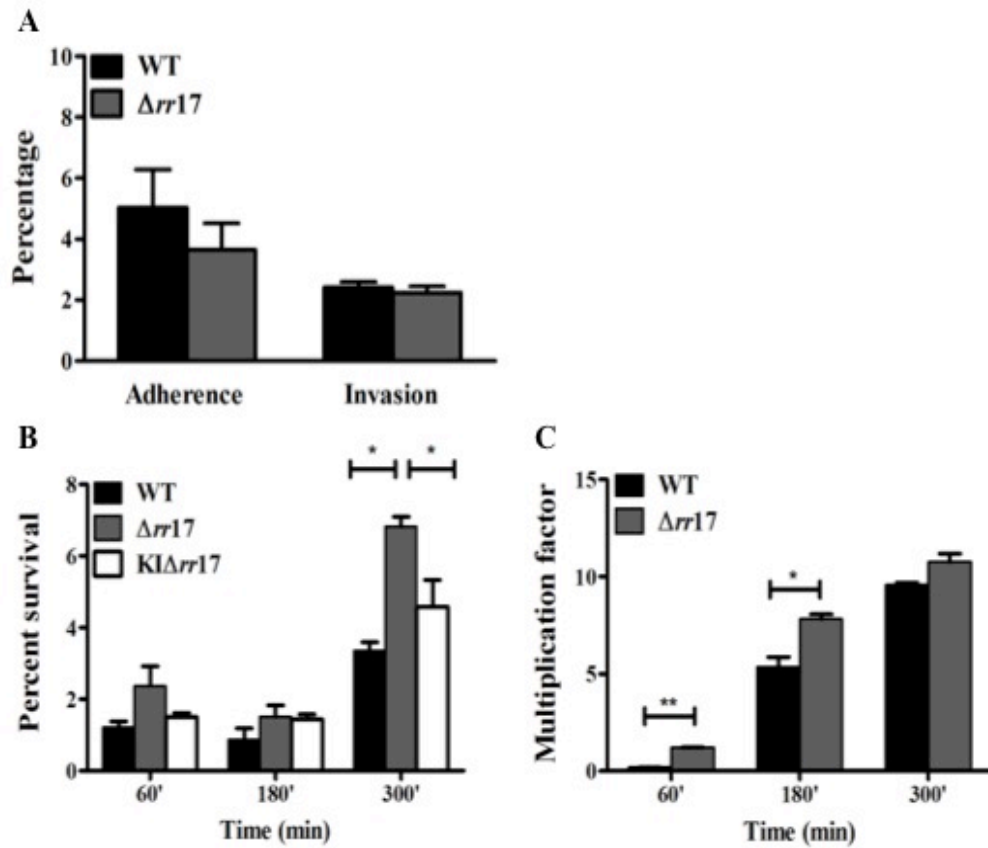


FIG 17 Adherence and invasion of hBMEC cells by WT and $\Delta rr17$ strains. Data are expressed as the total adherent CFU recovered compared to the input inoculum (MOI of 1; $\sim 1 \times 10^5$ CFU) (**A**). Percent survival of WT (black), $\Delta rr17$ (gray) and KI $\Delta rr17$ (white) in human blood. Data are expressed as the total CFU recovered compared to the input inoculum (**B**). Multiplication factor of WT (black) and $\Delta rr17$ (gray) in human plasma. Data are expressed as the total CFU recovered compared to the input inoculum (**C**). Triplicate samples were used and error bars show the SEM. Statistical analysis was performed by Student's T-test.

3. Discussion

In the present study, we conducted genome-wide inventory, classification, and comparative genomics of TCS in GBS, and can conclude that they are mostly conserved intra-species. For several of the TCS, putative orthologues were identified in other *Streptococcus* spp. For the remaining systems, the best hits were always identified in bacteria that are relatively close phylogenetically. However, the degree of sequence identity was more limited and closer scrutiny of gene context and domain architecture would be required to determine the likelihood of such TCS being true orthologues. Such an analysis could result in the identification of TCS that are unique for GBS biology. In our classification of sensing mechanisms, only one HK was classified as cytoplasmic sensing, while this is typically a more frequent category (16). A comparison of the number of TCS (corrected for genome size) in various pathogenic and non-pathogenic *Lactobacillales* spp. was also performed. In the nine species examined, GBS and *S. pyogenes* showed the highest frequency of TCS with a median of 38 and 36 TCS components respectively (data not shown), compared to a typical range of 15-32 for the other *Lactobacillales*. This suggests that the two pathogens may require particular fine-tuning of transcription in response to changing environments.

Transcriptome analysis was performed on five selected systems, and we observed a limited number of genes that were highly regulated for three TCS. TCS-2 regulates the adjacent *lrgAB* operon, similar to what has been described for *S. mutans* (35). TCS-11 regulates genes involved in purine metabolism and carbon starvation. TCS-16 highly regulates two PTS operons, and is discussed in more detail below.

TCS-17/RgfAC has already been described in GBS strain O90R, where it negatively regulates transcription of C5a peptidase (*scpB*), a known virulence factor (25). Moreover, an independent group demonstrated that in CC17 strains RgfAC negatively regulated the *fbxA* gene, encoding fibrinogen binding proteins (26). FbsA may have a role in protecting the bacteria against opsonophagocytosis, promoting adhesion to lung epithelial cells, and increasing survival in human blood (42, 43). We did not observe any up-regulation of the above genes in the $\Delta rr17$ strain, which may be due to differences in the experimental protocol (time points) or in the genetic background (CJB111 belongs to CC1 (44)). Nonetheless, the $\Delta rr17$ strain was hypervirulent in our murine model of systemic infection, consistent with a potential up-regulation of virulence factors in the absence of this transcriptional regulator.

The second system of particular interest was TCS-16. Transcriptome analysis showed prominent down-regulation of an adjacent operon that encodes a putative PTS (Man/Fru/Sor family) and concomitant up-regulation of another PTS (Fru family). TCS-16 was classified as an extracellular sensing system, and we hypothesized that it may be involved in monitoring and responding to the availability of nutrients (16). When bacteria were subjected to a large variety of different carbon sources in chemically defined medium, one compound, Fru-6-P, resulted in a complete growth defect, which was fully restored when the $\Delta rr16$ was complemented. Further experiments *in vitro*, using phosphorylated and non-phosphorylated hexose sugars confirmed these results. We thus conclude that a functional TCS-16 is necessary for growth on Fru-6-P. Investigation of the transcriptional events in the locus showed

that there is induction of TCS-16 upon exposure to extracellular Fru-6-P, and concomitantly a drastic up-regulation of the adjacent PTS operon. As the $\Delta rr16$ strain showed no such response, while the complemented strain exhibited a partial restoration, we conclude that a functional TCS-16 is necessary for autoinduction and regulation of the adjacent PTS operon. We propose that extracellular Fru-6-P is a signal for TCS-16, and that the gene locus be named *fspSR*, for fruse-six-phosphate sensor histidine kinase and response regulator. Despite the magnitude of the influence on PTS transcription, the growth defect observed in $\Delta rr16/\Delta fspR$ is difficult to explain in terms of a direct link between the up-regulated PTS and utilization of Fru-6-P as an energy source. To our knowledge, PTS-dependent import of phosphorylated sugars has not been described. However, other such uptake mechanisms are known, and UhpT (major facilitator superfamily) in *E. coli* represents an example where the controlling TCS (UhpAB) is necessary for growth of *E. coli* upon Glu-6-P and Fru-6-P (45, 46). We identified a homologue of UhpT in the genome of CJB111 (SAM1402), and analysis of the protein suggests it could function as a hexose-6-P transporter (<http://www.tcdb.org/>). SAM1402 was among the genes significantly down-regulated in the $\Delta rr16/fspR$ transcriptome and subsequent experiments confirmed that TCS-16/FspSR up-regulates *sam1402* in response to extracellular Fru-6-P. The biological relevance of our link between Fru-6-P and TCS-16/FspSR is difficult to ascertain, as the availability of Fru-6-P in the extracellular milieu is presumably limited or unknown. Nevertheless, our *in vivo* screening showed reduced vaginal persistence of the $\Delta rr16/\Delta fspR$ strain in mice, and a slight but

significant decrease in overall fitness when exposed to vaginal fluid components *ex vivo*. Interestingly, the presence of such unknown mucoidal components was necessary for survival/growth of the bacteria *in vitro*, when compared to the PBS control. PTS and associated carbon metabolism pathways may have an impact on *in vivo* fitness and virulence, as previously demonstrated for several different pathogens (47-51). One possibility is that Fru-6-P may be released from dying microorganisms in the complex microbiota of the vagina, or in stationary phase *in vitro* cultures, and GBS could consequently initiate a scavenging response involving up-regulation of sugar transporters. This hypothesis was supported by our data showing that there is an induction of the TCS-16 response upon exposure to bacterial lysate. This response was observed in the WT and complemented strains but not in the $\Delta rr16/\Delta fspR$ strain, confirming that a functional TCS-16 is necessary to up-regulate sugar transporters in the presence of lysed GBS components. Moreover in a previous work using a different strain, the PTS operon above, together with several other PTS were highly down-regulated in high-glucose conditions, supporting a role for this and similar systems in conditions where nutrients are relatively scarce (20). Another speculative possibility is that FspSR may be activated upon entry/invasion of eukaryotic cells, through the presence of Fru-6-P as a central metabolite in glycolysis.

We have listed and classified TCS in GBS for further study and conclude that these TCS are very well-conserved intra-species. Our results provide new insights on four previously unknown TCS, but also provide the first *in vivo* data supporting a role for RgfAC in virulence. Finally we identified FspRS, a new TCS involved in vaginal persistence and that responds to fructose-6-phosphate by the up-regulation of genes involved in sugar transport.

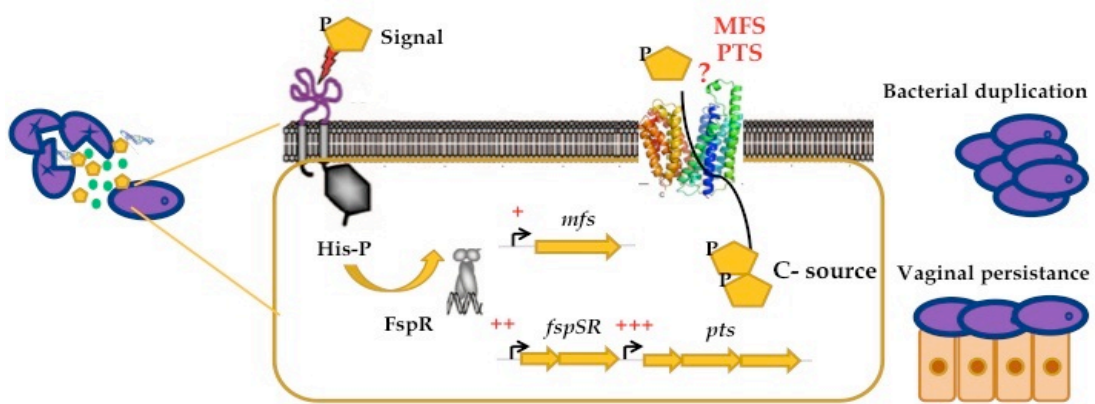


Fig.18 Model of TCS-16 working in response to Fru-6-P sugar.

4. Materials and Methods

4.1 Bacterial strains and growth conditions

GBS CJB111 (Carol Baker Collection, Division of Infectious Diseases, Baylor College of Medicine, Houston). and its isogenic derivatives were grown in Todd-Hewitt broth (THB medium; Difco Laboratories) at 37°C, 5% CO₂. Tryptic soy broth (Difco Laboratories), 15 g/L agar (TSA) was used as solid medium. MAX Efficiency® DH5α™ Competent Cells (Invitrogen) were used for transformation, propagation, and preparation of plasmids. *E. coli* was grown at 37°C with agitation (180 rpm) in Luria-Bertani (LB, Difco laboratories) broth, or on 15 g/L agar plates (LBA) Erythromycin (Erm) was used for selection of GBS (1 µg/ml) or *E. coli* (100 µg/ml) containing the pJRS233-derived plasmids used for mutagenesis (see below).

Strains CJB111, CJB111Δ*rrl6* and CJB111KI*rrl6* were also grown in CDM (36), or CDM where glucose was substituted with 10 g/L glucose-6-phosphate, fructose, fructose-6-phosphate, mannose or mannose-6-phosphate (Sigma). Briefly, bacteria grown on THB plates were suspended in 5 ml of PBS until optical density at 600 nm (OD₆₀₀) reached 0.3. Samples were then diluted 1:10 in PBS and 88 µl of bacteria were added to 1.2 ml of medium with or without different carbon sources. Bacteria were grown in 96-well plates with 200 µl per well for 48 h at 37°C and OD₆₀₀ was monitored automatically every 20 min in an automated reader (Sunrise, Tecan).

4.2 Construction of TCS isogenic mutants

To construct each knock out strain, the shuttle vector pJRS233 (52) containing the TCS locus with an in-frame deletion in the response regulator gene (*rr*) was constructed using a splicing by overlap extension PCR (SOEing-PCR) strategy (Table 4) (53). Briefly, the up- and downstream region of a *rr* gene were produced from CJB111 gDNA and then joined. The resulting fragment was cloned into pJRS233 using BamHI and XhoI restriction sites.

Five plasmids, each containing an insert with 700-800 bp upstream and downstream of the in-frame deleted *rr* gene were obtained: pJRS233 Δ *rr2*, pJRS233 Δ *rr11*, pJRS233 Δ *rr16*, pJRS233 Δ *rr17* and pJRS233 Δ *rr21*. The CJB111 genes thus inactivated were SAM0184 (*rr2*), SAM1027 (*rr11*), SAM1885 (*rr16*), SAM1897 (*rr17*), and SAM2044 (*rr21*).

To construct the respective chromosomally complemented knock-in (KI) strains, the wild type locus was amplified and cloned into pJRS233 using BamHI and XhoI restriction sites (Table 4). These plasmids were designated pJRS233KI*rr2*, pJRS233KI*rr11*, pJRS233KI*rr16*, pJRS233KI*rr17* and pJRS233KI*rr21*.

An insertion/duplication and excision mutagenesis strategy was used to obtain either the in-frame deletion in the response regulator genes or the chromosomal replacement in the knockout mutants. In brief, pJRS233 Δ *rr2*/ Δ *rr11*/ Δ *rr16*/ Δ *rr17*/ Δ *rr21* purified from *E. coli* were used to transform CJB111 by electroporation as previously described (54), except that we used M9 medium without glycine and casamino acids. Transformants were selected by growth on TSA + Erm at 30°C for 48 hours. Integration was performed by growth of transformants at 37°C (non-permissive

temperature for the suicide shuttle vector) with Erm selection. Excision of the integrated plasmid was performed by serial passages in THB at 30°C, and parallel screening for Erm-sensitive colonies on plate. Mutants were verified by PCR sequencing of the TCS loci. We thus obtained five knockout strains, each having an inactivated response regulator gene of a specific TCS: CJB111 Δ *rr2*, CJB111 Δ *rr11*, CJB111 Δ *rr16*, CJB111 Δ *rr17* and CJB111 Δ *rr21*. Or, in short, Δ *rr2* etc.

To obtain the chromosomally complemented strains, plasmids PJRS233K*Irr2*/K*Irr11*/K*Irr16*/K*Irr17*/K*Irr21* were purified from *E. coli* and complementation of the respective mutant strains was performed as described above. The end result was replacement of the deleted *rr* gene with the WT form. The complemented strains were designated CJB111K*Irr2*; CJB111K*Irr11*; CJB111K*Irr16*; CJB111K*Irr17*; CJB111K*Irr21*. Or, in short, K Δ *rr2* etc.

4.3 Recombinant RR16 cloning, expression and purification

The expression plasmids pET15TEV (Novagen) and pMAL-c4X (Invitrogen vector modified in house) were used to clone the rRR16 protein fused respectively with a His tag and a His-MBP-TEV tag at its N-terminal region. Plasmids were previously modified in house to clone proteins using the PIPE strategy (55). Briefly, *rr* gene was produced from CJB111 gDNA (i-PCR). Plasmids were linearized by PCR (v-PCR), mixed with the insert in a ratio of 1:3 and used to transform *E. coli* HK-100 competent cells (Table 4). The resulting constructs were analyzed by DNA

sequencing and expressed in *E. coli* T7 express (pET15TEV-rRR16-His) (Invitrogen) or *E. coli* BL21(DE3) (pMal-rRR16-MBP-His) cells resistant to phage T1 (NEB).

The cells were grown in EnBase (Biosilta) medium in shaking flasks at 30°C for 16 hours of cultivation, until OD₆₀₀ about 15, and then induced with 1 mM IPTG for 2 hours (pET15TEV-rRR16-His) or 8 hours (pMal-rRR16-MBP-His) at 25°C. Afterwards the cells were harvested by centrifugation at 6000 rpm for 30 min. The soluble proteins were extracted using the cell lytic buffer (Sigma) and centrifuged 40 min at 9000 rpm to remove the cell debris. Protein affinity purification was performed on a FF-Crude His-Trap HP nickel chelating column (GE Healthcare) pre-equilibrated with the binding buffer (Tris-HCl (pH=8) 20 mM, NaCl 300 mM, Imidazole 10 mM).

The proteins were eluted with 300 mM imidazole; at the end of the Immobilized Metal Ion Affinity Chromatography (IMAC) all the fractions obtained were analyzed by SDS-PAGE.

For the pMal-rRR16-MBP-His purification, the eluted protein was concentrated by ultrafiltration with amicon (Millipore) and the buffer was exchanged using a PD-10 desalting column (GE Healthcare) equilibrated with TEV cleavage buffer (Tris-HCl 50 mM (pH 8), DTT 1 mM, EDTA 0.5 mM). His-MBP-tag was cleaved by incubation with TEV protease. The second step of purification was performed by size exclusion chromatography using HiLoad 26/60 Superdex 200 (GE Healthcare) equilibrated in Tris-HCl 25 mM (pH=8) and NaCl 150 mM. The proteins were quantified with the BCA assay (Pierce).

4.4 Bioinformatics methods

The identification of histidine kinases (HKs) and response regulators (RRs) of putative TCS in the genome of GBS 2603 V/R was carried out using the P2CS (<http://www.p2cs.org>) database (31). A TCS was defined as an orphan if the predicted HK or RR genes had no adjacent partner in the locus, or if the cognate partner contained mutations (e.g. stop codons or frameshifts) that compromised the predicted gene product.

Orthologue analysis was performed by using the BLASTp algorithm with default settings on complete and draft genomes of GBS strains A909, 515, H36b, NEM316, 18rs21, COH1 and CJB111 (21-23). Loci encoding putative orthologues were examined manually for the gene context, which in the vast majority of cases was identical. The orthologues identified were then examined manually for detection of polymorphisms that would result in significant alterations of the gene product. Overall sequence quality was also inspected, and the presence of ambiguous nucleotides or a contig break within 100 bp of a polymorphism was taken as an indication of questionable sequence quality. HK and RR proteins from 2603 V/R were then used as queries in a BLASTp search of a database of non-redundant protein sequences, and the best non-GBS hits were examined. The best ‘combined hit’ was defined as the cognant HK/RR pair in one species with the lowest product of the two corresponding individual E values.

Functional domains in each HK protein were identified by SMART and/or PFAM (<http://smart.embl-heidelberg.de>). Subsequently, HKs were manually assigned a signaling mechanism according to proposed criteria (16). Extracellular sensing HKs

typically have two TM helices with an intervening extracytoplasmic domain of 50 to 300 aa, lacking large cytoplasmic linker regions; transmembrane sensing HK are characterized by the presence of 2 to 20 transmembrane regions connected by very short intra- or extracellular linkers; cytoplasmic-sensing HKs include either membrane-anchored proteins that do not fulfill the criteria above and where input domains (e.g. PAS, GAF) are localized on the intracellular side, or, soluble HKs with no transmembrane regions.

4.5 Expression microarray analysis

Expression microarray analysis was performed using a custom-made Agilent 60-mer oligonucleotide microarray. Oligonucleotide sequences were selected with the Agilent eArray system, using 6 probes per gene. The complete set of annotated genes (2,232) in the CJB111 genome was thus covered (<http://cmr.jcvi.org/cgi-bin/CMR/GenomePage.cgi?org=gbscjb111>). The chip layout was submitted to the EBI ArrayExpress and is available with the identifier AMEX-BBB. RNA samples used for microarray analysis were prepared as follows. Bacteria for RNA extraction were grown in triplicate cultures (five mutant strains and the isogenic WT strain), on three separate occasions. Hence, for each strain, nine independent GBS cultures (nine biological replicates obtained in three separate days) served as the source of RNA. Bacteria were harvested twice: at $OD_{600}=0.3$ (EL phase) and $OD_{600}=1.8-1.9$, (ES phase, ~ 15 min into growth arrest). To rapidly arrest transcription, 10 ml of bacteria were cooled on ice and added to 10 ml of frozen THB medium in a 50 ml conical tube. GBS cells were then collected by centrifugation for 15 min at 4000 rpm, 4°C,

and resuspended in 800 μ l of TRIzol (Invitrogen). Bacteria were disrupted mechanically by agitation with Lysing matrix B in 2 ml tubes (DBA Italy) using a homogenizer (Fastprep-24, Millipore) for 60 sec at 6.5 m/s for two cycles, and kept on ice for 2 min between the cycles. Samples were then centrifuged for 5 min at 8000 x g, 4°C and RNA was extracted with Direct-zol™ RNA MiniPrep kit (Zymo Research) according to the manufacturer's instructions. RNA samples were treated with DNase (Roche) for 2 h at 37°C and further purified using the RNA MiniPrep kit (Qiagen), including a second DNase treatment on the column for 30 min at room temperature (RT), according to the manufacturer's instructions. 5 μ g of pooled RNA from each triplicate were labeled (CY5-DCTP/CY3-DCTP, Euroclone) and purified (Wizard®SV Gel and PCR Clean-Up System; Promega). RNA thus labeled from the three independent days of RNA extraction was then pooled and used for microarray analysis. Labeling, chip hybridization, wash, scanning and data extraction were performed according to the procedures described by Agilent for two-color microarray-based gene expression analysis. After data acquisition, slide normalization was performed by a lowess (locally weighted scatterplot smoothing) algorithm, as implemented by the Agilent Feature Extraction software v.9.5.3. Average log ratio of fluorescence signals ($M = \log_2(\text{Cy5}/\text{Cy3})$) of probes corresponding to the same gene were computed within each slide. Student's T-test statistics was performed to test for differentially expressed genes. The expression dataset was submitted to the EBI ArrayExpress and it is available with the identifier AMEXP-CCC.

4.6 qRT-PCR analysis

cDNA was prepared using the Reverse Transcription System (Promega) by using 500 ng of RNA per reaction. Real time quantitative PCR (qRT-PCR) was performed on 50 ng of cDNA that was amplified using LightCycler[®] 480 DNA SYBR Green I Master, (Roche). Reactions were monitored using a LightCycler[®] 480 instrument and software (Roche). The transcript amounts in each condition were standardized to an internal control gene (*gyrA*) and compared with standardized expression in the wild-type strain ($\Delta\Delta C_T$ method). Validation of microarray data by qRT-PCR was performed on a selection of 9 genes differentially expressed in mutant strains, using the RNA prepared for microarray analysis (see above) and primers reported in Table 4. Moreover, we prepared new RNA samples from WT, knock-out and complemented strains (three biological replicates obtained in three different days) to generate cDNA for qRT-PCR confirmation of highly regulated genes.

For RNA extraction from bacteria grown with different carbon sources, strains were first inoculated in CDM and grown at 37°C until $OD_{600}=0.5$. Cultures were harvested by centrifuging at 4000 x g, 4° C, for 10 min, and each pellet was resuspended in 10 ml of CDM (36) without glucose and split in two. Each 5 ml sample was then supplemented with 10 mg/ml of glucose or fructose-6-phosphate. Bacteria were then incubated for 30 min at 37°C and RNA was extracted as described for the microarray analysis.

Bacterial lysate was obtained from a 10 ml culture of the WT strain in late logarithmic phase (OD=1). Briefly, bacteria resuspended in PBS were disrupted mechanically by agitation with Lysing matrix B in 2 ml tubes (DBA Italy) using a homogenizer (Fastprep-24, Millipore) for 60 sec at 6.5 m/s for four cycles. Tubes were kept on ice for 2 min between the cycles. Samples were centrifuged for 5 min at 8000 x g, 4°C and the supernatant was collected and designated lysate. For the RNA extraction, strains were grown in CDM until OD₆₀₀=0.5, harvested, split in two, and resuspended in 5 ml of CDM without glucose. Each sample was supplemented with 800 µl of PBS or with 800 µl of lysate for 30 min at 37°C before RNA extraction.

4.7 Phenotype Microarray analysis

Phenotype Microarray (PM) technology uses the irreversible chemical reduction of a patented dye as a reporter of active metabolism (56). Strains CJB111, $\Delta rr16$ and $KIrr16$, were used with microplates PM1 and PM2A (Biolog), testing 192 different single carbon sources. Bacteria on THB agar plates were scraped off and suspended in 5 ml of inoculation fluid (IF-0; Biolog) to an OD=0.3. Samples were then diluted 1:10 in IF-0 to obtain a turbidity of 85% (OD~0.02-0.03), and kept on ice. Growth media constituents were prepared according to Biolog's procedures for '*S. agalactiae* and other Streptococcus species'. PM microplates were inoculated by adding 100 µl bacterial suspension/well and then incubated for 48 h at 37°C in an OmniLog reader (Biolog). Data points were collected every 15 min. Data were then analyzed using the

OmniLog software. Unspecific background (well A1 in each plate, negative control) was subtracted from the other samples.

4.8 *In vivo* infection experiments

Animal studies were approved by the Office of Lab Animal Care at San Diego State University and conducted under accepted veterinary standards. Animal experiments were performed in compliance with the Novartis Animal Health & Welfare guidelines. We adopted a previously described murine model of hematogenous GBS meningitis (41), with the difference that preliminary dose-ranging experiments established the LD₅₀ dose of CJB111 as 1.5×10^7 CFU per mouse (outbred 6-week old male CD1, Charles River laboratories). The mice were followed for 2 weeks. Also, since histopathology was not performed, we thus considered the experiment a model of systemic infection.

The *in vivo* mouse model of GBS vaginal colonization has been described previously (39). Female CD1 mice (8-16 weeks old) were obtained from Charles River Laboratories and used for colonization assays.

4.9 *In vitro* infection experiments

The immortalized human vaginal epithelial cell (HVEC) line was obtained from the American Type Culture Collection 129 (ATCC CRL-2616) (57). *In vitro* adhesion was performed as previously described (39) and passages 5-10 were used for all cell assays. Cells were maintained at 37°C in a 5% CO₂ atmosphere in keratinocyte serum-free medium (KSFM) (Invitrogen).

The human brain microvascular endothelial cell line hBMEC, which has been immortalized by transfection with the SV40 large T antigen (58), was obtained from Kwang Sik Kim (Johns Hopkins University, Baltimore, Maryland, USA). hBMEC maintain the morphologic and functional characteristics of primary brain endothelial cells (59, 60). The cells were maintained in RPMI 1640 medium (Life Technologies Inc., Grand Island, New York, USA) supplemented with 10% FBS, 10% NuSerum (Becton, Dickinson and Co., Bedford, Massachusetts, USA), MEM nonessential amino acids, and penicillin-streptomycin and were incubated at 37°C in 5% CO₂. Cell maintenance and assays for GBS hBMEC adherence, invasion, and intracellular survival were performed as described previously (60, 61). For all experiments, hBMECs were used at passage 8–14.

4.10 *Ex vivo* GBS growth experiments

Growth of CJB111 and CJB111 Δ *rr16* was assessed *ex vivo* in murine vaginal lavage fluid. Lavage fluid was collected from female CD1 mice (8 weeks old) without any GBS exposure by pipetting 20 μ L of PBS into the vaginal lumen several times. Lavage fluid was pooled and stored at -20°C. Bacterial strains were grown to exponential phase (approximately 1×10^8 CFU/mL) in THB, washed, diluted 1:100 in PBS, and 90 μ L was combined with 10 μ L vaginal lavage fluid. Samples were collected at indicated time points and plated on THB agar to determine viable CFU.

Growth of CJB111; CJB111 Δ *rr17* and CJB111KI Δ *rr17* was assessed *ex vivo* in human blood and human plasma. Blood was freshly collected from one donor the

morning of the experiment. All strains to be tested were grown on TS agar plates at 37°C and 5% CO₂ overnight. Bacteria were inoculated in THB liquid medium to an OD of 0.05 at 600 nm and grown to early-log phase (OD of 0.5–0.6); then, they were concentrated to ~10⁹ CFU/ml in PBS. The assay was started by the addition of the bacterial suspension (10 µL~10⁷ CFU) to 100% whole human blood (340 µL) in 2 ml tubes. Cultures were incubated at 37°C and 5% CO₂ with gentle agitation; at various time points (30, 60, 180 and 300 minutes), an aliquot of the sample was removed, and the number of viable bacteria was determined by plating serial dilutions onto TS Agar (Difco) and incubating overnight at 37°C and 5% CO₂.

Experiments were performed in duplicate. Whole venous blood, collected from healthy individuals and anticoagulated with heparin (5 U/mL), was used.

Survival in human plasma was performed using human plasma collected from human blood after centrifugation at 1000 x g, 4°C for 15 minutes in 15 ml tubes. The experiment was then performed as described for the one in human blood.

4.11 Oligo list

Oligo name ^a	Sequence (5' to 3') ^b	Application
F184soe1	CTGGGATCCGGGATAACAGAGGAACAA	mutagenesis <i>rr2</i>
R184soe1	ACCTACTGGGGCAAACATTTTCATCATCAAGAAT	mutagenesis <i>rr2</i>
F184soe2	ATGTTTGCCCCAGTAGGTCGATCGTATTTAAAA	mutagenesis <i>rr2</i>
R184soe2	TGACTCGAGCCAAAAGAATGACAATACCACT	mutagenesis <i>rr2</i>
F1027soe1	AAGGATCCGATCACATGCTTCATTGACTT	mutagenesis <i>rr11</i>
R1027soe1	TATTGTATGCGCTCTTACATTGTGAACATTAAT	mutagenesis <i>rr11</i>
F1027soe2	GTAAGAGCGCATAACAATACCTTTCTAATTTTAAAT	mutagenesis <i>rr11</i>
R1027soe2	TTCTCGAGGCACAACATATGACTTACGTT	mutagenesis <i>rr11</i>
F1885soe1	AACGGATCCACCCTTTTTTGCAAATTGAC	mutagenesis <i>rr16</i>
R1885soe1	GATGAGGGTCAGACAGTAAAAGCGTTT	mutagenesis <i>rr16</i>
F1885soe2	TGTCTGACCCTCATCCTCAACGATAAGTAATCT	mutagenesis <i>rr16</i>
R188 soe2	CACTCGAGCTGGTCGCTCTTTTTTCTCTA	mutagenesis <i>rr16</i>
F1897soe1	TAGGATCCCTCAATATGGTGGCTATAATC	mutagenesis <i>rr17</i>
R1897soe1	CAGGCAGGTTCGAATTGTTTGTATTTCTCGT	mutagenesis <i>rr17</i>
F1897soe2	ATTCGAACCTGCCTGTTGAATAAAATTATCCTC	mutagenesis <i>rr17</i>
R1897soe2	ATACTCGAGCTGAAACCATTAAGCCAGAT	mutagenesis <i>rr17</i>
F2044soe1	TATGGATCCCCTTCCCTACCGTAATAAAGGT	mutagenesis <i>rr21</i>
R2044soe1	TTTACCACCGGGGTCATCATCAATAATATAGAA	mutagenesis <i>rr21</i>
F2044soe2	GACCCCGGTGGTAAAATTTCACTTAAACGTTTT	mutagenesis <i>rr21</i>
R2044soe2	TTGCTCGAGCTTACCTTCTTAATAACACAAAT	mutagenesis <i>rr21</i>
F183	GTCAGTTACGCGCAGTTCAA	qRT-PCR
R183	GCCTCTTATAATTTGCAAACG	qRT-PCR
F1028	CCTGTTCCAATTCATCATGAAGA	qRT-PCR
R1028	GGATAGCGAAAAAGCAAGAAAG	qRT-PCR
F1886	GATGCGATCGCTAGAAGT	qRT-PCR
R1886	CACGATCATCGAGCTTTTGTG	qRT-PCR
F1896	GTCGGAAATGTGATTAGATTCTT	qRT-PCR
R1896	CCACCATAATTGAGGGGTTGT	qRT-PCR
F2045	GGTCAACTTCAGCCGTCAA	qRT-PCR
R2045	GTGAACGTCGCCGAAATAT	qRT-PCR
F1888	CCGCAAACCATCAAGGTAAC	qRT-PCR
R1888	TCAGGTTTTGAGGAATATGATGG	qRT-PCR
F1715	GGTCCCATTTGAGCCTTTAC	qRT-PCR
R1715	TTCAATGGTCTCCTCAAGGTC	qRT-PCR
F0011	TGTCATTGAAGCGACAGCTC	qRT-PCR
R0011	AACGCTCTGCCTGTTTATCC	qRT-PCR
F1026	TGGTTTCCATGCTACCCAAG	qRT-PCR
R1026	CTGCAATCATCATGCCGTAG	qRT-PCR
F1800	TTACAGCATGCGGAAACG	qRT-PCR
R1800	TTTTGCTTCTCCGACTGAGC	qRT-PCR
F1061	TGCTCTAGGATTGGACGTTTG	qRT-PCR
R1061	GTGATTGGCTTGGATGTTGG	qRT-PCR
F0185	TCACTACCAATCCCAACGAC	qRT-PCR
R0185	AAGCCCCAAAAGAGTCAACC	qRT-PCR
F1402	TCGGACTTCCGCCTATAGAA	qRT-PCR
R1402	TACAAGGATGCCACATCAG	qRT-PCR
F0012	TGACCCTAATGCCTTTCTGTC	qRT-PCR
R0012	ACTTCGCCAGGTTCAACATC	qRT-PCR
F0064	CGTGTTGGTTTTGGTACAGG	qRT-PCR
R0064	CGTGAGGAATTGTTGTACCG	qRT-PCR
F1059	TGCAGAGCAAATCGGGTATC	qRT-PCR
R1059	TTAACCCTTCGTCGTGATG	qRT-PCR
F0965	AGGTTTACTTGTGGCGCTTG	qRT-PCR- <i>gyrA</i>
R0965	TCTGCTTGAGCAATGGTGTC	qRT-PCR- <i>gyrA</i>
F1885Pipe	CTGTACTIONCAGGGCTATAGATTACTTATCGTTGAGGATGAGCAC	PIPE-iPCR
R1885Pipe	AAATTAAGTCGCGTTAATCCATCTGTTTAAAAAATATGTTCTTCTTAAAC	PIPE-iPCR
FpMal	TAACGCGACTTAATTTAACTTAATTAATTAATTAATTAATTAATTCAGAATTCGGA	PIPE-vPCR
RpMal	GCCCTGGAAGTACAGGCCCTGGAAGTACAGGTTTTTC	PIPE-vPCR
FpET	TAACGCGACTTAATTTCTAGCATAACCCCTTGGGGCCTCAAACGG	PIPE-vPCR
RpET	GCCCTGGAAGTACAGGTTTTCTGTGATGATGATGATGATGATGGCTGCTGCC	PIPE-vPCR
	ATGGTATATC	

TABLE 4: ^a Numbers refer to the CJB111 gene designations (<http://cmr.jcvi.org>); ^b BamHI and XhoI restriction sites (underlined) and complementary nucleotides used for PCR SOEing or for PIPE (bold) are shown.

References

1. **Baker CJ, Clark DJ, Barrett FF.** 1973. Selective broth medium for isolation of group B streptococci. *Appl Microbiol* **26**:884–885.
2. **Brown JH.** 1937. Appearance of Double-Zone Beta Hemolytic Streptococci in Blood Agar. *J. Bacteriol.* **34**:35–48.
3. **Franciosi RA, Knostman JD, Zimmerman RA.** 1973. Group B streptococcal neonatal and infant infections. *J Pediatr* **82**:707–718.
4. **Howard JB, McCracken GH.** 1974. The spectrum of group B streptococcal infections in infancy. *Am. J. Dis. Child.* **128**:815–818.
5. **Finch LA, Martin DR.** 1984. Human and bovine group B streptococci: two distinct populations. *J Appl Bacteriol* **57**:273–278.
6. **Dermer P, Lee C, Eggert J, Few B.** 2004. A history of neonatal group B *Streptococcus* with its related morbidity and mortality rates in the United States. *J Pediatr Nurs* **19**:357–363.
7. **Sendi P, Johansson L, Norrby-Teglund A.** 2008. Invasive group B Streptococcal disease in non-pregnant adults : a review with emphasis on skin and soft-tissue infections. *Infection* **36**:100–111.
8. **Rubens CE, Wessels MR, Heggen LM, Kasper DL.** 1987. Transposon mutagenesis of type III group B *Streptococcus*: correlation of capsule expression with virulence. *Proceedings of the National Academy of Sciences of the United States of America* **84**:7208–7212.

9. **Wessels MR, Rubens CE, Benedí VJ, Kasper DL.** 1989. Definition of a bacterial virulence factor: sialylation of the group B streptococcal capsule. *Proceedings of the National Academy of Sciences of the United States of America* **86**:8983–8987.
10. **Marques MB, Kasper DL, Pangburn MK, Wessels MR.** 1992. Prevention of C3 deposition by capsular polysaccharide is a virulence mechanism of type III group B streptococci. *Infection and Immunity* **60**:3986–3993.
11. **Takahashi S, Aoyagi Y, Adderson EE, Okuwaki Y, Bohnsack JF.** 1999. Capsular sialic acid limits C5a production on type III group B streptococci. *Infection and Immunity* **67**:1866–1870.
12. **Rajagopal L.** 2009. Understanding the regulation of Group B Streptococcal virulence factors. *Future Microbiol* **4**:201–221.
13. **Fernandez M, Rench MA, Albanyan EA, Edwards MS, Baker CJ.** 2001. Failure of rifampin to eradicate group B streptococcal colonization in infants. *Pediatr Infect Dis J* **20**:371–376.
14. **Maisey HC, Doran KS, Nizet V.** 2008. Recent advances in understanding the molecular basis of group B *Streptococcus* virulence. *Expert reviews in molecular medicine* **10**:e27.
15. **Foussard M, Cabantous S, Pédelacq J, Guillet V, Tranier S, Mourey L, Birck C, Samama J.** 2001. The molecular puzzle of two-component signaling cascades. *Microbes Infect.* **3**:417–424.
16. **Mascher T, Helmann JD, Unden G.** 2006. Stimulus perception in bacterial signal-transducing histidine kinases. *Microbiology and molecular biology*

reviews : MMBR 70:910–938.

17. **Glaser P, Rusniok C, Buchrieser C, Chevalier F, Frangeul L, Msadek T, Zouine M, Couvé E, Lalioui L, Poyart C, Trieu-Cuot P, Kunst F.** 2002. Genome sequence of *Streptococcus agalactiae*, a pathogen causing invasive neonatal disease. *Mol. Microbiol.* **45**:1499–1513.
18. **Tettelin H, Masignani V, Cieslewicz MJ, Eisen JA, Peterson S, Wessels MR, Paulsen IT, Nelson KE, Margarit I, Read TD, Madoff LC, Wolf AM, Beanan MJ, Brinkac LM, Daugherty SC, Deboy RT, Durkin AS, Kolonay JF, Madupu R, Lewis MR, Radune D, Fedorova NB, Scanlan D, Khouri H, Mulligan S, Carty HA, Cline RT, Van Aken SE, Gill J, Scarselli M, Mora M, Iacobini ET, Brettoni C, Galli G, Mariani M, Vegni F, Maione D, Rinaudo D, Rappuoli R, Telford JL, Kasper DL, Grandi G, Fraser CM.** 2002. Complete genome sequence and comparative genomic analysis of an emerging human pathogen, serotype V *Streptococcus agalactiae*. *Proceedings of the National Academy of Sciences of the United States of America* **99**:12391–12396.
19. **Jiang SM, Ishmael N, Dunning Hotopp J, Puliti M, Tissi L, Kumar N, Cieslewicz MJ, Tettelin H, Wessels MR.** 2008. Variation in the group B *Streptococcus* CsrRS regulon and effects on pathogenicity. *J. Bacteriol.* **190**:1956–1965.
20. **Di Palo B, Rippa V, Santi I, Brettoni C, Muzzi A, Metruccio MME, Grifantini R, Telford JL, Paccani SR, Soriani M.** 2012. Adaptive Response of Group B *Streptococcus* to High Glucose Conditions: New Insights on the

CovRS Regulation Network. PLoS One **8**:e61294–e61294.

21. **Lamy MC, Zouine M, Fert J, Vergassola M, Couve E, Pellegrini E, Glaser P, Kunst F, Msadek T, Trieu-Cuot P, Poyart C.** 2004. CovS/CovR of group B *Streptococcus* : a two-component global regulatory system involved in virulence. Mol. Microbiol. **54**:1250–1268.
22. **Jiang S-M, Cieslewicz MJ, Kasper DL, Wessels MR.** 2005. Regulation of virulence by a two-component system in group B *Streptococcus*. J. Bacteriol. **187**:1105–1113.
23. **Poyart C, Lamy MC, Boumaila C, Fiedler F, Trieu-Cuot P.** 2001. Regulation of D-alanyl-lipoteichoic acid biosynthesis in *Streptococcus agalactiae* involves a novel two-component regulatory system. J. Bacteriol. **183**:6324–6334.
24. **Poyart C, Pellegrini E, Marceau M, Baptista M, Jaubert F, Lamy M-C, Trieu-Cuot P.** 2003. Attenuated virulence of *Streptococcus agalactiae* deficient in D-alanyl-lipoteichoic acid is due to an increased susceptibility to defensins and phagocytic cells. Mol. Microbiol. **49**:1615–1625.
25. **Spellerberg B, Rozdzinski E, Martin S, Weber-Heynemann J, Luttkicken R.** 2002. *rgf* encodes a novel two-component signal transduction system of *Streptococcus agalactiae*. Infection and Immunity **70**:2434–2440.
26. **Safadi Al R, Mereghetti L, Salloum M, Lartigue M-F, Virlogeux-Payant I, Quentin R, Rosenau A.** 2010. Two-component system RgfA/C activates the *fbsB* gene encoding major fibrinogen-binding protein in highly virulent CC17 clone group B Streptococcus. PLoS One **6**:e14658–e14658.

27. **Quach D, van Sorge NM, Kristian SA, Bryan JD, Shelver DW, Doran KS.** 2009. The CiaR response regulator in group B *Streptococcus* promotes intracellular survival and resistance to innate immune defenses. *J. Bacteriol.* **191**:2023–2032.
28. **Rozhdestvenskaya AS, Totolian AA, Dmitriev AV.** 2010. Inactivation of DNA-binding response regulator Sak189 abrogates beta-antigen expression and affects virulence of *Streptococcus agalactiae*. *PLoS One* **5**:e10212.
29. **Klinzing DC, Ishmael N, Dunning Hotopp JC, Tettelin H, Shields KR, Madoff LC, Puopolo KM.** 2013. The two-component response regulator LiaR regulates cell wall stress responses, pili expression and virulence in group B *Streptococcus*. *Microbiology* **159**:1521–1534.
30. **Zaleznik DF, Rench MA, Hillier S, Krohn MA, Platt R, Lee ML, Flores AE, Ferrieri P, Baker CJ.** 2000. Invasive disease due to group B *Streptococcus* in pregnant women and neonates from diverse population groups. *Clinical infectious diseases : an official publication of the Infectious Diseases Society of America* **30**:276–281.
31. **Barakat M, Ortet P, Jourlin-Castelli C, Ansaldi M, Méjean V, Whitworth DE.** 2008. P2CS: a two-component system resource for prokaryotic signal transduction research. *BMC Genomics* **10**:315–315.
32. **Galperin MY.** 2010. Diversity of structure and function of response regulator output domains. *Curr. Opin. Microbiol.* **13**:150–159.
33. **Tettelin H, Massignani V, Cieslewicz MJ, Donati C, Medini D, Ward NL, Angiuoli SV, Crabtree J, Jones AL, Durkin AS, Deboy RT, Davidsen TM,**

- Mora M, Scarselli M, Margarit y Ros I, Peterson JD, Hauser CR, Sundaram JP, Nelson WC, Madupu R, Brinkac LM, Dodson RJ, Rosovitz MJ, Sullivan SA, Daugherty SC, Haft DH, Selengut J, Gwinn ML, Zhou L, Zafar N, Khouri H, Radune D, Dimitrov G, Watkins K, O'Connor KJ, Smith S, Utterback TR, White O, Rubens CE, Grandi G, Madoff LC, Kasper DL, Telford JL, Wessels MR, Rappuoli R, Fraser CM.** 2005. Genome analysis of multiple pathogenic isolates of *Streptococcus agalactiae*: implications for the microbial “pan-genome.” Proceedings of the National Academy of Sciences of the United States of America **102**:13950–13955.
34. **Ahn S-J, Qu M-D, Roberts E, Burne RA, Rice KC.** 2011. Identification of the *Streptococcus mutans* LytST two-component regulon reveals its contribution to oxidative stress tolerance. BMC Microbiol **12**:187–187.
35. **Ahn S-J, Rice KC, Oleas J, Bayles KW, Burne RA.** 2010. The *Streptococcus mutans* Cid and Lrg systems modulate virulence traits in response to multiple environmental signals. Microbiology **156**:3136–3147.
36. **van de Rijn I, Kessler RE.** 1980. Growth characteristics of group A streptococci in a new chemically defined medium. Infection and Immunity **27**:444–448.
37. **Watson MEJ, Nielsen HV, Hultgren SJ, Caparon MG.** 2013. Murine vaginal colonization model for investigating asymptomatic mucosal carriage of *Streptococcus pyogenes*. Infection and Immunity **81**:1606–1617.
38. **Patras KA, Wang NY, Fletcher EM, Cavaco CK, Jimenez A, Garg M, Fierer J, Sheen TR, Rajagopal L, Doran KS.** 2013. Group B *Streptococcus*

- CovR regulation modulates host immune signalling pathways to promote vaginal colonization. *Cell Microbiol* **15**:1154–1167.
39. **Sheen TR, Jimenez A, Wang NY, Banerjee A, van Sorge NM, Doran KS.** 2011. Serine-rich repeat proteins and pili promote *Streptococcus agalactiae* colonization of the vaginal tract. *J. Bacteriol.* **193**:6834–6842.
 40. **Doran KS, Engelson EJ, Khosravi A, Maisey HC, Fedtke I, Equils O, Michelsen KS, Arditi M, Peschel A, Nizet V.** 2005. Blood-brain barrier invasion by group B *Streptococcus* depends upon proper cell-surface anchoring of lipoteichoic acid. *J Clin Invest* **115**:2499–2507.
 41. **Doran KSK, Liu GYG, Nizet VV.** 2003. Group B streptococcal beta-hemolysin/cytolysin activates neutrophil signaling pathways in brain endothelium and contributes to development of meningitis. *J Clin Invest* **112**:736–744.
 42. **Schubert A, Zakikhany K, Pietrocola G, Meinke A, Speziale P, Eikmanns BJ, Reinscheid DJ.** 2004. The fibrinogen receptor FbsA promotes adherence of *Streptococcus agalactiae* to human epithelial cells. *Infection and Immunity* **72**:6197–6205.
 43. **Schubert A, Zakikhany K, Schreiner M, Frank R, Spellerberg B, Eikmanns BJ, Reinscheid DJ.** 2002. A fibrinogen receptor from group B *Streptococcus* interacts with fibrinogen by repetitive units with novel ligand binding sites. *Mol. Microbiol.* **46**:557–569.
 44. **Springman AC, Lacher DW, Wu G, Milton N, Whittam TS, Davies HD, Manning SD.** 2009. Selection, recombination, and virulence gene diversity

- among group B streptococcal genotypes. *J. Bacteriol.* **191**:5419–5427.
45. **Webber CA, Kadner RJ.** 1997. Involvement of the amino-terminal phosphorylation module of UhpA in activation of *uhpT* transcription in *Escherichia coli*. *Mol. Microbiol.* **24**:1039–1048.
 46. **Zhou L, Lei XH, Bochner BR, Wanner BL.** 2003. Phenotype microarray analysis of *Escherichia coli* K-12 mutants with deletions of all two-component systems. *J. Bacteriol.* **185**:4956–4972.
 47. **Barelle CJ, Priest CL, Maccallum DM, Gow NAR, Odds FC, Brown AJP.** 2006. Niche-specific regulation of central metabolic pathways in a fungal pathogen. *Cell Microbiol* **8**:961–971.
 48. **Tchawa Yimiga M, Leatham MP, Allen JH, Laux DC, Conway T, Cohen PS.** 2006. Role of gluconeogenesis and the tricarboxylic acid cycle in the virulence of *Salmonella enterica* serovar Typhimurium in BALB/c mice. *Infection and Immunity* **74**:1130–1140.
 49. **Munoz-Elias EJ, McKinney JD.** 2005. Mycobacterium tuberculosis isocitrate lyases 1 and 2 are jointly required for *in vivo* growth and virulence. *Nature medicine* **11**:638–644.
 50. **Lau GW, Haataja S, Lonetto M, Kensit SE, Marra A, Bryant AP, McDevitt D, Morrison DA, Holden DW.** 2001. A functional genomic analysis of type 3 *Streptococcus pneumoniae* virulence. *Mol. Microbiol.* **40**:555–571.
 51. **Polissi A, Pontiggia A, Feger G, Altieri M, Mottl H, Ferrari L, Simon D.** 1998. Large-scale identification of virulence genes from *Streptococcus*

- pneumoniae. *Infection and Immunity* **66**:5620–5629.
52. **Perez-Casal J, Price JA, Maguin E, Scott JR.** 1993. An M protein with a single C repeat prevents phagocytosis of *Streptococcus pyogenes*: use of a temperature-sensitive shuttle vector to deliver homologous sequences to the chromosome of *S. pyogenes*. *Mol. Microbiol.* **8**:809–819.
 53. **Horton RM, Hunt HD, Ho SN, Pullen JK, Pease LR.** 1989. Engineering hybrid genes without the use of restriction enzymes: gene splicing by overlap extension. *Gene* **77**:61–68.
 54. **Framson PE, Nittayajarn A, Merry J, Youngman P, Rubens CE.** 1997. New genetic techniques for group B streptococci: high-efficiency transformation, maintenance of temperature-sensitive pWV01 plasmids, and mutagenesis with Tn917. *Appl Environ Microbiol* **63**:3539–3547.
 55. **Klock HE, Lesley SA.** 2009. The Polymerase Incomplete Primer Extension (PIPE) method applied to high-throughput cloning and site-directed mutagenesis. *Methods Molecular Biology* **498**.
 56. **Bochner BR, Gadzinski P, Panomitros E.** 2001. Phenotype microarrays for high-throughput phenotypic testing and assay of gene function. *Genome Res.* **11**:1246–1255.
 57. **Fichorova RN, Rheinwald JG, Anderson DJ.** 1997. Generation of papillomavirus-immortalized cell lines from normal human ectocervical, endocervical, and vaginal epithelium that maintain expression of tissue-specific differentiation proteins. *Biol. Reprod.* **57**:847–855.
 58. **Stins MF, Prasadarao NV, Zhou J, Arditi M, Kim KS.** 1997. Bovine brain

microvascular endothelial cells transfected with SV40-large T antigen: development of an immortalized cell line to study pathophysiology of CNS disease. *In Vitro Cell. Dev. Biol. Anim.* **33**:243–247.

59. **Huang SH, Stins MF, Kim KS.** 2000. Bacterial penetration across the blood-brain barrier during the development of neonatal meningitis. *Microbes Infect.* **2**:1237–1244.
60. **Kim KS.** 2001. *Escherichia coli* translocation at the blood-brain barrier. *Infection and Immunity* **69**:5217–5222.
61. **Nizet V, Kim KS, Stins M, Jonas M, Chi EY, Nguyen D, Rubens CE.** 1997. Invasion of brain microvascular endothelial cells by group B streptococci. *Infection and Immunity* **65**:5074–5081.

Ringraziamenti

Vorrei ringraziare tutti coloro che mi hanno aiutata, sostenuta e supportata durante questi quattro anni contribuendo non solo alla realizzazione di questo progetto di tesi, ma anche alla mia formazione scientifica e personale.

In primis ringrazio il Dott. Robert Janulczyk, per la sua guida scientifica, l'affetto e la pazienza dimostrata.

La ricerca è un percorso arduo e dietro ogni successo sono celati cento e più insuccessi. E' facile, quindi, comprendere come l'umore e la motivazione possano risentirne quando sforzi e sacrifici personali non vedono il loro giusto appagamento. Mentirei, dunque, negando che in questi anni non ci siano stati momenti di sconforto e abbattimento, momenti in cui mi sono chiesta se ne valesse la pena e se questa fosse la mia strada. Sono stati questi i momenti in cui il mio gruppo e le mie amiche mi hanno maggiormente aiutato. Ringrazio quindi il Dott. Matteo M. Metruccio, per essermi stato vicino prima come amico e poi come mentore scientifico. Ringrazio Chiara Toniolo, per aver reso il nostro laboratorio un ambiente familiare ed accogliente. Ringrazio le mie amiche Alessia Corrado, Nunzia D'Urzo, Francesca Zerbini, Lorenza

Tulli e Buket Baddal per esserci sempre state, ricordandomi il mio valore e la mia passione tutte le volte che li dimenticavo.

Ringrazio Emiliano Chiarot, punto di riferimento indispensabile, mentore impagabile, amico fidato e consigliere esperto, senza il quale la mia crescita non sarebbe stata completa.

Ringrazio il Dott. Manuele Martinelli, la Dott.ssa Roberta Cozzi, la Dott.ssa Maria Giuliani e la Dott.ssa Valentina Rippa, per i loro insegnamenti scientifici, il loro affetto e la loro disponibilità.

In fine, un ringraziamento speciale va alla mia project leader, Immaculada Margarit Y Ros, che mi ha permesso di svolgere questo lavoro di tesi e che ha sempre dato prova di credere in me.

In questi anni ho capito che se, nonostante le mille difficoltà, è sufficiente un piccolo successo per ritrovare il giusto spirito e la giusta motivazione, allora è veramente questo il tuo percorso. E', infatti, quel piccolo successo la fiamma che alimenta lo spirito del ricercatore, rigenerando quell'entusiasmo e quell'energia necessarie per proseguire lungo la strada della conoscenza. D'altronde, nessuno ha detto che sarebbe stato facile, hanno solo promesso che ne sarebbe valsa la pena (Harvey MacKay).

Special acknowledgment Dott. Kelly S.Doran. The experience in her lab changed the way I look at science. Thanks to her I learned that science is fun, that the only way to become a good scientist is by comparing and listening and that new people can always teach you something, even if they are younger. In three months she became my friend and her lab my family. Moreover she helped and sponsored me when I was looking for a postdoctoral position in USA. Thanks to her I found the path I want to follow and I will continue my scientific growth in the American Academia.

She is my model: an extraordinary woman, a great scientist, a big leader and a wonderful mother, and she is on the top of everything she does.

Thanks Kelly!